Vagus nerve stimulation recruits the central cholinergic system to enhance perceptual learning

Kathleen A. Martin[1-5], Eleni S. Papadoyannis[6], Jennifer K. Schiavo[1-4], Saba Shokat Fadaei[1-4], Sofia Orrey Valencia[1-4], Nesibe Z. Temiz[7], Matthew J. McGinley[8-9], David A. McCormick[10], Robert C. Froemke[1-5,*]

[1] Skirball Institute for Biomolecular Medicine, New York University School of Medicine, New York, NY, USA

[2] Neuroscience Institute, New York University School of Medicine, New York, NY, USA

[3] Department of Otolaryngology, New York University School of Medicine, New York, NY, USA

[4] Department of Neuroscience and Physiology, New York University School of Medicine, New York, NY, USA

[5] Center for Neural Science, New York University, New York, NY, USA

[6] Princeton Neuroscience Institute, Princeton University, Princeton, New Jersey

[7] Friedrich Miescher Institute for Biomedical Research, Basel, Switzerland

[8] Duncan Neurological Research Institute, Baylor College of Medicine, Houston TX 77030

[9] Department of Neuroscience, Baylor College of Medicine, Houston TX 77030

[10] Institute of Neuroscience, University of Oregon, Eugene OR 97403

* correspondence to: robert.froemke@med.nyu.edu

Abstract

Perception can be refined by experience up to certain limits. It is unclear if perceptual limitations are absolute or could be partially overcome via enhanced neuromodulation and/or plasticity. Recent studies suggest the utility of peripheral nerve stimulation - specifically vagus nerve stimulation (VNS) - for altering neural activity and augmenting experience-dependent plasticity, although little is known about central mechanisms recruited by VNS. Here we developed an auditory discrimination task for mice implanted with a VNS electrode. VNS occurring during behavior gradually improved discrimination abilities beyond the level achieved by training alone. Using two-photon imaging, we identified changes to auditory cortical responses and activation of cortically-projecting cholinergic axons with VNS. Anatomical and optogenetic experiments indicated that VNS could enhance task performance via activation of the central cholinergic system. These results highlight the importance of cholinergic modulation for the efficacy of VNS, perhaps enabling further refinement of VNS methodology for clinical conditions.

Introduction

Sensory processing is refined over development and must continue to be adaptive throughout life, in order to adequately regulate behavior in dynamic and challenging environments. This requires that adult perceptual and cognitive abilities are not fixed, but rather can be improved with additional experience and training. Perceptual learning, i.e., improvement in sensory perceptual abilities with practice, has been shown to occur across a wide range of domains, including visual processing of orientation, binocularity, and other spatial features[1–7], auditory processing of pitch and temporal intervals[8–12], and the detection and recognition of sensory stimuli in other modalities[13–15]. However, changes in perceptual abilities can often be quite limited and stimulus-specific, even after extensive periods of training[5,16–18]. It is generally believed that adult perceptual learning across species relies on neural mechanisms of synaptic plasticity within the cerebral cortex[1,7,14,17], but it remains unclear what factors might limit cortical plasticity achieved by perceptual training and any consequent changes in perception and behavior. Conversely, mechanisms for plasticity not engaged during training might then be available for recruitment by other means, and perhaps improve sensory perceptual abilities even further.

Studies of the mammalian auditory system have proved to be especially revealing for determining the mechanisms connecting perceptual learning and neural plasticity. A long literature has connected changes in auditory experience with long-lasting neural changes in the central auditory system. In particular, many studies have demonstrated how auditory training affects tonotopic maps and single neuron responses, showing that acoustic stimuli predictive of outcome generally have enhanced representations in the auditory cortex[8,9,11,12,19,20]. Despite clear evidence that behavioral training eventually affects cortical maps and receptive fields, it is less clear how these

37 changes are initially induced and occur throughout experience and learning to produce perceptual
38 changes[21,22]. One consistent finding across systems and species is that central neuromodulatory
39 systems such as the cholinergic basal forebrain are important for sensory perceptual learning and
40 cortical plasticity[23–38]. However, it remains unclear the extent to which modulatory systems are
41 endogenously recruited under different contexts or forms of training, and if it might be possible to
42 artificially leverage central modulation to further improve perceptual learning.
43
44 Peripheral nerve stimulation provides an opportunity to augment performance and lead to lasting
45 improvements in auditory perceptual abilities via activation of neuromodulatory systems. Vagus
46 nerve stimulation (VNS) has been used for several clinical applications in humans, including
47 treating epilepsy[39,40], alleviating treatment-resistant depression[41], and motor deficits after stroke [42].
48 Despite its well-established benefits, less is known about the circuit mechanism through which
49 VNS acts. This has led to experimental approaches for studying VNS in a range of species
50 including rats[43,44], ferrets[45], and non-human primates[46]. Recently, in collaboration we developed
51 and validated a VNS cuff electrode for mice[47–50] to investigate the role of neuromodulation in
52 VNS-mediated motor and perceptual learning. Previous work in non-human model organisms has
53 shown that vagus nerve stimulation can induce neuroplasticity in primary sensory areas[43,44,51] and
54 in motor areas[50,52,53]. This enhanced neuroplasticity is thought to be partially mediated by
55 indirectly activating neuromodulatory networks, including noradrenergic neurons in locus
56 coeruleus[49,54,55] and cholinergic neurons in basal forebrain[48–50] via the nucleus tractus solitarii
57 (NTS) [56,57]. With the development of VNS cuffs for mice, we aimed to study the circuit
58 mechanisms and modulatory systems activated by VNS, asking how VNS might be applied to
59 promote plasticity and improve auditory perceptual learning.
60

Results

Auditory perceptual training in head-fixed mice

We first developed an auditory task to parametrically quantify the psychophysical abilities of mice for frequency discrimination. A total of 38 mice (5 female wild-type, 11 male wild-type, 8 female ChAT-Cre, 14 male ChAT-Cre) were used for behavioral studies. Animals were head-fixed and progressively trained to classify presented pure tones in a two-alternative forced-choice (2AFC) task for a water reward. On each trial, mice were presented with an auditory stimulus of one frequency ranging between 4-38 kHz at 70 dB sound pressure level (SPL). Mice were trained to lick left in response to tones of one specific 'center' frequency (varied between 11-16 kHz across individual animals), and to lick right for tones of any other 'non-center' frequency in a 2.5s response period (**Fig. 1a**, **Extended Data Fig. 1a,b**, lick rates were significantly higher in the 1 second following tone offset, N=6 mice). There were eight non-center tones with four tones up to 1.5 octaves lower than the center frequency, and four tones up to 1.5 octaves higher than the center frequency in the full training set (**Fig. 1b**).

Mice learned the task in three stages, with additional frequencies added as individual performance improved. During stage 1 (first shaping stage), we only presented two frequencies (the 'center' tone and one 'non-center' tone 1.5 octaves from center; **Fig. 1b**, light blue). Animals completed stage 1 after reaching our performance criterion (≥80% correct) for three consecutive days (**Fig. 1c**). The number of days to reach performance criteria in stage 1 was variable across individual mice, from 5-37 days (**Fig. 1d,e**). There were no significant differences in performance across stage one by sex or genotype (wild-type vs ChAT-Cre in C57Bl/6J background; wild-type males: 10.8±3.8 days in stage 1, mean±s.d., N=11; wild-type females: 16.4±7.7 days, N=5; ChAT-Cre

84 males: 10.1±3.9 days, N=14; ChAT-Cre females: 7.8±5.4 days, N=8; p=0.05 for genotype, p=0.62
85 for sex, two-way ANOVA with Tukey's multiple comparisons correction). Following stage 1, we
86 then introduced one other 'non-center' frequency that was 1.5 octaves away from the center
87 frequency in the opposite direction (**Fig. 1b**, medium blue), and trained animals in this second
88 shaping stage for three days (**Fig. 1c,d**). We then introduced all other frequencies (stage 3; **Fig.**
89 **1c,d**, N=38 mice), with all animals being trained in stage 3 for at least nine days (**Extended Data**
90 **Fig. 1c**). Overall performance plateaued at days 7-9 of stage 3, but was variable across individuals
91 (**Extended Data Fig. 1d,e,f**, peak performance was not significantly correlated with total days
92 trained in stage 3, Pearson's R=0.31, minimum five days of training prior to baseline; Days 0-2:
93 64.7±1.0%; Days 6-8: 70.0±1.2%; Max day ± 1 day: 72.6±1.3%, Mean±s.d.; $p<10^{-4}$ one-way
94 ANOVA with Tukey's multiple comparisons correction, N=38 animals). Performance improved
95 across non-center frequencies throughout stage 3 with the largest improvement occurring at the
96 frequencies ±0.5 octaves from center (**Fig. 1f**, N=38 mice, day 1 of stage 3 compared to maximum
97 performance, minimum of 3 days of stable performance, **Extended Data Fig. 1g,h**).
98
99 Task performance varied considerably across animals even after days to weeks of training (**Fig.**
100 **1f, Extended Data Fig. 1e,f,g,h**). On the day of peak performance, animals correctly identified
101 frequencies as the center frequency at 84.5±12.7% of the time (N=38 animals, mean±s.d.,
102 minimum 3 days of stable performance). Animals generally had stable performance across days
103 after at least nine days in the full version of the task (**Fig. 1g**). Even after performance stabilized,
104 most animals continued to make a significant number of errors on the non-center frequencies
105 closest to the center, either a quarter octave or a half octave away from the center frequency (**Fig.**
106 **1h**; error rates at ±0.25 octaves: 67.6±19.0%; error rates at ±0.5 octaves: 45.2±20.6%, mean±s.d.;

107 significantly higher errors compared to center tone responses, $p<10^{-5}$, one-way ANOVA with
108 Tukey's multiple comparisons correction).
109
110 We explored if there was a discrimination threshold further by overtraining a subset of mice for
111 36.3±12.4 days in stage three (**Extended Data Fig. 2a**, range: 21-48 days, N=6). We then altered
112 the reward structure of the task, such that all errors had a larger impact on the amount of water the
113 mice received. Specifically, we increased the magnitude of reward for all trials (from ~3μL to
114 ~6μL) and reducing the overall number of trials (from 400 to 200) for an additional 12-13 days of
115 behavior (**Extended Data Fig. 2b**). There was no significant improvement in performance at the
116 center frequencies or frequencies ±0.25 and ±0.5 octaves from center when comparing all days
117 with the increased reward size and the five finals days with smaller rewards (**Extended Data Fig.**
118 **2c,d,e,** at 0: small reward: 78.9±4.1% correct, mean±s.e.m., large reward: 83.5±3.3%, p=0.15,
119 Student's two-tailed paired t-test; at ±0.25: small reward: 36.9±6.8%, large reward: 35.4±4.3%,
120 mean±s.e.m.; p=0.67, Student's two-tailed paired t-test; at ±0.5: small reward: 64.2±7.0% correct,
121 large reward: 71.4±6.3%, mean±s.e.m.; p=0.08, Student's two-tailed paired t-test). These data
122 show that while head-fixed mice have relatively stable frequency discrimination abilities,
123 performance remained imperfect even after many days of continued positive reinforcement to
124 correctly resolve frequencies within 0.25-0.5 octaves[35,58,59].
125
126 **Long-term vagus nerve stimulation in mice**
127 Our behavioral results showed that, once a certain level of performance was obtained, additional
128 training did not consistently refine perceptual abilities in an individual animal beyond a certain
129 level. This is consistent with a substantial literature on psychophysics and perceptual learning in

130 humans and other species[5,16–18,35]. We wondered if this was a fixed perceptual limit (e.g., set by
131 physical limitations of the sensory epithelium) or if it could be improved by engagement of central
132 mechanisms of neuromodulation and plasticity. Methods such as transgene expression and
133 optogenetic stimulation can lead to lasting behavioral gains in rodents[21], but these approaches are
134 currently infeasible or impractical in many species including human subjects. However,
135 stimulation of the vagus nerve has recently been shown to influence neural responses in the central
136 nervous system, altering physiological and cognitive variables[41,43,54,55,60]. Some of these effects
137 may be due to indirect activation of central modulation, but little is known about the underlying
138 mechanisms by which VNS initiates prolonged enhancement of behavior.
139
140 We adapted the bipolar VNS cuff used in rats[43] to make custom vagus nerve cuff electrodes for
141 use in mice[47–49] and verified successful stimulation of the vagus nerve by measuring impedance of
142 the cuff electrode. We implanted custom cuff electrodes around the left vagus nerve in adult mice
143 (**Fig. 2a**). We measured cuff impedance daily in awake animals for days to months post-
144 implantation over the course of behavioral training (**Extended Data Fig. 3a,b**). Cuff impedances
145 <10 kΩ were considered potentially viable for VNS, and many animals had stable cuff impedances
146 in this range for weeks (**Extended Data Fig. 3b**). We used change in heart rate as a physiological
147 signature for effective VNS (**Extended Data Fig. 3c-f**). When cuff impedance values were very
148 high (e.g., ~100 MΩ; **Extended Data Fig. 3d**), VNS was ineffective at affecting physiological
149 variables such as heart rate, consistent with our previous work[47]. We thus defined as sham
150 implantations either those electrodes for which impedance values were over 10 kΩ and/or cases in
151 which VNS did not elicit significant changes in heart rate (**Extended Data Fig. 3f**, 7/10 animals

with viable cuffs <10kΩ had significantly lower heart rate distributions in sessions with 500 ms of VNS every 10s than in sessions without VNS).

Vagus nerve stimulation improves auditory perceptual learning over days

We next asked how VNS might affect the performance of fully trained animals on the 2AFC task. After several days of training on stage 3 (average 14.8+/-8.4 days, range 6-36 days), we implanted 17 animals with a vagus nerve cuff. Of the animals implanted, seven trained mice had <10 kΩ cuff impedances and VNS elicited changes in heart rate (**Extended Data Fig. 3**) and were subsequently included and analyzed as part of the experimental group. All other animals were part of the sham-implanted control group (N=10). Experimental and control animals did not have any significant differences in baseline performance, including peak performance, response rate, and learning rate (**Extended Data Fig. 4a,b,c,d,e**). After implantation, animals recovered for about a week with *ad lib* water, and training on the 2AFC task was reinstated after 4-10 days of additional water restriction (total days in stage 3: average 19.0±8.5 days, range 10-40 days). Prior to the start of VNS pairing, implanted animals were trained for 3-7 days post-implantation without VNS, to establish a new baseline level of performance and ensure that this was comparable to their pre-implantation behavior (**Extended Data Fig. 4f**, change in performance (experimental): -1.8±1.6% correct, mean±s.e.m., p=0.38, Student's two-tailed paired t-test, N=7; change in performance (control): 0.4±1.0% correct, mean±s.e.m., p=0.68, Student's two-tailed paired t-test, N=10 mice; p=0.28 for experimental and control comparison, Student's two-tailed unpaired t-test). VNS occurred during behavior in a blockwise manner, with a 'block' being a set of 50 trials. In blocks 1, 3, and 5 there was no VNS, and training was identical to that previously described in **Figure 1**. In blocks 2 and 4, VNS was performed concurrently with tone presentation, essentially being

175 paired with all center and non-center stimuli. Specifically, we stimulated the vagus nerve for 500
176 ms at 30 Hz with a 100 μs pulse width centered around the 250 ms tone, such that VNS began 125
177 ms before tone onset and continued for 125 ms after tone offset (**Fig. 2b**). By design, this meant
178 that VNS pairing was performed irrespective of trial outcome, in contrast to a recent important
179 study of motor learning[50]. For experimental animals, VNS stimulation intensity was 0.6-0.8 mA,
180 fixed per animal. For sham-implanted, control animals, VNS stimulation intensity varied from 0
181 to 0.8 mA. Animals underwent VNS pairing for 20 consecutive days.
182
183 We found that VNS pairing led to enduring improvements in 2AFC task performance for most
184 animals, which emerged gradually over days and largely enhanced correct responses to the ±0.25
185 and ±0.5 octave flanking non-center tones (**Fig. 2c**). We initially quantified the change in
186 performance across all stimuli over all five training blocks ('Δ % correct') as the overall correct
187 rate on each day relative to the average performance on the final three days of training prior to
188 pairing initiation. Given there was a significant increase in response rate in experimental animals
189 relative to control animals (**Extended Data Fig. 5a,b,c,d)**, we included no response trials for
190 comparisons between experimental and control animals. The maximum change in 2AFC task
191 performance occurred several days after initiating VNS pairing during training (**Fig. 2c**, peak
192 performance after 15.4±2.8 days, mean±s.d., N=7 mice). We compared behavioral performance
193 on the final three days of VNS pairing (day 18-20) to the baseline behavioral performance on the
194 three days of training just before the start of VNS pairing in experimental and sham-implanted
195 control animals. Behavioral performance significantly increased in experimental animals (**Fig. 2d**,
196 N=7 mice, before VNS: 65.4±2.8% correct over all center/non-center stimuli, including no
197 response trials (day 18-20 of VNS: 77.1±3.1% correct over all stimuli, p=0.008, Student's two-

198 tailed paired t-test), but not in sham control animals (**Fig. 2d**, N=10 mice, before VNS: 68.5±2.4%
199 correct, day 18-20 of VNS: 67.4±2.8% correct over all stimuli, p=0.65, Student's two-tailed paired
200 t-test). Experimental animals had a significantly larger improvement in performance than sham
201 animals (**Fig. 2e**, mean difference in performance (experimental): 11.7±3.0% correct, mean±s.e.m;
202 mean difference (sham): -1.1±2.4% correct, mean±s.e.m., N=10, p=0.002, Student's one-tailed
203 unpaired t-test).
204
205 As VNS occurred with presentation of both center and non-center stimuli, we asked if performance
206 at certain frequencies were specifically improved after days of VNS pairing (**Fig. 2f**, all 17 sham
207 and experimental animals individually displayed in **Extended Data Fig. 5e**). We noticed that, on
208 average, behavioral performance improved at both the center frequency (**Fig. 2f,g**, Day -2-0:
209 71.6±7.0%, mean±s.e.m.; Day 18-20: 84.9±5.0%, p=0.02, Student's two-tailed paired t-test) and
210 the non-center tones flanking the center (**Fig. 2f**; ±0.25 and ±0.5 octaves from center). To correct
211 for perceptual improvements at the center frequency across animals, we normalized the behavioral
212 performance at individual frequencies on the final days of VNS pairing (days 18-20) and baseline
213 performance (**Fig. 2h-k**, N=7 experimental mice; N=10 control mice). Most of the improvement
214 in behavioral performance came from gradual reductions in errors at non-center frequencies ±0.25
215 and 0.5 octave from the center frequency in experimental animals compared to control animals
216 (**Fig. 2h**). The reduction of normalized errors, and resulting improved performance, at frequencies
217 ±0.25-0.5 octaves from center (**Fig. 2h-j**, 'Experimental', for ±0.25: p=0.04, Student's two-tailed
218 paired t-test; for ±0.5: p=0.01, N=7) were not observed for ±0.25-0.5 octave stimuli in control
219 animals receiving sham VNS (**Fig. 2h-j**,'Sham', for ±0.25: p=0.13, Student's two-tailed paired t-
220 test; for ±0.5: p=0.81, Student's two-tailed paired t-test, N=10 mice). Additionally, the reduction

221 in errors between the final days of VNS (days 18-20) and the three days immediately prior were
222 significantly reduced in experimental animals relative to control animals at frequencies ±0.5
223 octaves from center (**Fig. 2k**, for ±0.5: p=0.002, Student's one-tailed unpaired t-test).
224
225 As the behavioral effects of VNS pairing gradually emerged over several days, we wondered if
226 there were also immediate, acute perceptual effects during the paired training sessions, and/or if
227 there were improvements occurring each day from block to block with successive training within
228 a daily session. We first analyzed behavioral differences across blocks with and without VNS
229 pairing, specifically comparing block one and three (without VNS) vs block two and four (with
230 VNS). We focused on these two blocks of trials to capture potential differences, e.g., in
231 motivational state as animals acquired more water rewards. In sessions with blocks of VNS,
232 performance did not selectively improve during VNS pairing blocks compared to unpaired blocks,
233 across all stimuli in experimental (**Fig. 3a**; block one performance without VNS: 79.5±3.2%
234 correct, mean±s.e.m.; block two performance with VNS: 79.1±1.9%,; block three performance
235 without VNS: 77.6±3.4%; block four performance with VNS: 75.8±2.5%; N=7, p=0.78, one-way
236 ANOVA with Tukey's multiple comparisons correction), or sham-implanted control animals (**Fig.
237 3a**; open circles, block one performance without VNS: 73.3±2.7% correct, mean±s.e.m.; block two
238 performance with VNS: 65.5±4.6%; block three performance without VNS: 70.9±3.5%; block four
239 performance with VNS: 64.9±4.8%,; p=0.37, one-way ANOVA with Tukey's multiple
240 comparisons correction; N=10). Similarly, there was no significant change in performance
241 between blocks with and without VNS for experimental and control animals (**Fig. 3b**; difference
242 in experimental animals: -1.1±1.3% lower in sessions without VNS, mean±s.e.m.; difference in
243 control animals: -6.9±3.8% lower in sessions without VNS, p=0.23, Student's two-tailed unpaired

244 t-test). There also could be rapid changes in motivation, learning, or other aspects of animal state
245 within a session from block to block independent of VNS pairing. To account for this, we
246 compared performance per block in the three initial baseline sessions prior to initiating VNS
247 pairing. We found that performance was stable across all blocks in these baseline sessions (**Fig.**
248 **3c**; block one performance: 68.0±4.3% correct, mean±s.e.m.; block two performance: 63.9±3.6%
249 correct; block three performance: 63.1±3.7% correct; block four performance: 63.7±3.4%; N=7,
250 p=0.78, one-way ANOVA with Tukey's multiple comparisons correction). Additionally, there was
251 no significant change in performance across specific frequencies in blocks with or without VNS
252 in experimental or control animals (**Fig. 3d,e**, p=0.28 for frequencies, p=0.11 for experimental
253 group, two-way ANOVA with Tukey's multiple comparisons correction). There was also no
254 significant change in response rate across blocks in both experimental and control animals (**Fig.**
255 **3f,g**; experimental means: block one response rate: 97.1±2.0%; block two: 98.2±1.6%; block three:
256 95.0±3.0%; block four: 95.5±2.8%; N=7, p=0.77, one-way ANOVA with Tukey's multiple
257 comparisons correction; control means: block one response rate: 96.7±1.6%; block two:
258 91.9±3.8%; block three: 93.9±2.1%; block four: 85.7±5.7%; N=10, p=0.20, one-way ANOVA
259 with Tukey's multiple comparisons correction).
260
261 Instead of immediate gains in performance during or just after VNS pairing, these results indicate
262 that behavioral changes took days to emerge, accruing over daily sessions with VNS pairing. This
263 would suggest that the gradual changes in performance might be observed even in block one across
264 days, before any VNS pairing occurred on that day. To test this hypothesis, we compared
265 performance on block one (i.e., the first 50 2AFC trials without VNS pairing of each day) to
266 performance over all blocks across days. Experimental animals exhibited similar rates of

267 improvement over time for block one alone compared to performance on all trials following block
268 1 (**Fig. 3h-j**). Across animals, the change in performance during block one of the final days of
269 VNS was significantly correlated with change in performance over all other trials (**Fig. 3l**,
270 Pearson's R=0.78, p=0.008). In contrast, control animals did not exhibit the same significant
271 improvements in performance in block one (**Fig. 3j-l**).
272
273 **VNS pairing enables long-term cortical plasticity**
274 Our results demonstrate that VNS pairing enhanced perceptual learning even beyond the limits
275 achieved just by behavioral training. As these gains emerged gradually over days, we suspected
276 that a mechanism related to enduring neuroplasticity was being engaged by VNS pairing. Previous
277 studies in rats pairing pure tones with VNS[43,51] found changes to neuronal populations and
278 tonotopic maps of primary auditory cortex (A1), strongly suggesting that auditory cortex is a locus
279 of potentially behaviorally-relevant plasticity.
280
281 To identify possible long-term changes in cortical responses and receptive fields triggered by VNS
282 pairing, we performed longitudinal two-photon imaging in mouse auditory cortex of seven
283 untrained animals (**Fig. 4a**; 6 wild-type females, 1 wild-type male). We injected all mice with a
284 CaMKII-GCaMP6f in auditory cortex, waited 2-4 weeks for viral expression, and then implanted
285 a VNS cuff electrode on the left vagus nerve. We paired a tone of a single frequency with VNS by
286 coincidental presentation every 2.5 seconds for 5 minutes each day for at least 5 days (up to 20
287 days). We performed these experiments outside the context of behavior, so that we could monitor
288 neural changes that might be more directly attributed to VNS-mediated plasticity, avoiding the
289 confound of cortical plasticity that might occur due to training[8,9,11,12]. In each animal, we tracked

290 a consistent population of neurons over days of pairing (**Fig. 4a-c**, **Extended Data Fig. 6**). We
291 also presented pure tones of 4-64 kHz every 1-3 days throughout the pairing procedure to monitor
292 changes across a wider frequency range of the receptive fields (**Fig. 4a**). Additionally, after the
293 initial pairing session, we presented the same set of frequencies both 15 minutes and 2 hours after
294 VNS pairing to look for more acute changes of auditory responses in a subset of animals. In control
295 animals (1 wild-type female, 3 wild-type males), we performed the same pairing protocol,
296 presenting a tone of a single frequency every 2.5 seconds, but without coincident VNS (**Fig. 4a**).
297 Changes in tuning were assessed in the same manner.
298
299 We imaged from layer 2/3 excitatory neurons in each animal (N=7 mice, 144.8±33.2 neurons per
300 animal, mean±s.d.) in a 300 μm x 300 μm region. 455/1081 neurons (42.1%) recorded prior to
301 VNS-tone pairing were responsive to at least one frequency between 4-64 kHz, and 371/953
302 neurons (37.8%) recorded on day 5 of pairing were responsive (with 465 cells imaged on both
303 sessions). There was no change in the percentage of significantly responsive neurons across days
304 and type of pairing (sham or experimental pairing) (**Fig. 4d,** p=0.96 for experimental animals,
305 p=0.20 for sham animals, Student's paired t-test, p=0.11 for difference across time points for
306 experimental and sham animals, Student's unpaired t-test). For each animal, we computed the
307 overall best frequency across auditory cortex in the region of imaging (initial best frequency, 'Pre
308 peak'), and 78/455 responsive neurons (17.1%) on the first imaging day had significant or maximal
309 responses to that local best frequency. We then chose a frequency that was initially under-
310 represented at the level of individual neuronal tuning profiles as the 'paired frequency', with
311 29/455 responsive neurons (6.4%) initially responding to that frequency across animals before
312 VNS pairing.

313

314 VNS pairing modified the tuning curves of auditory-responsive cells over minutes to days, as
315 quantified by the percentage of active neurons responding to a certain stimulus (**Fig. 4e-g**). We
316 measured the change in number of responsive neurons at three frequencies: the initial best
317 frequency ('Pre peak'; black), the paired frequency ('P', blue), and a frequency one octave from
318 the paired frequency ('±1', gray) to ask how stimulus-specific these changes were. We focused
319 our analysis of frequency receptive fields to several time points throughout pairing, trying to
320 highlight any plasticity that could occur over minutes to hours (**Fig. 4h,i**) or over days (**Fig. 4j-l**).
321 Since there was significant individual variability in reaching peak behavioral improvement, we
322 postulated that a similar variability could be present in VNS-mediated long-term plasticity across
323 animals. To that end, we looked at the number of days it took animals to show maximal changes
324 at the paired frequency (**Fig. 4k,l**).

325

326 At shorter time scales (15 minutes post initial pairing, **Fig. 4h**, 2 hours post initial pairing, **Fig. 4i**),
327 there were not significant changes in response to the paired frequency ('P', blue), initial best
328 frequency ('Pre peak', black), or the frequency one octave away from the paired frequency (±1,
329 gray). However, consistent with the gradual time course of behavioral enhancement we observed
330 with VNS, reliable and lasting cortical changes required several days to emerge. At both long-term
331 time points (after five days of pairing and the day with maximal changes at the paired frequency),
332 two major changes resulted from VNS pairing but not control pairing (**Fig. 4j-l**). First, the overall
333 number of neurons responding to the paired frequency significantly increased (Day 5:
334 113.3±132.2% increase at paired frequency, mean±s.d., one-way ANOVA with Tukey's multiple
335 comparisons correction; response at paired frequency was significantly different than 'Pre peak'

with $p<0.05$; Max: 263.2±295.2% increase; mean±s.d., response at paired frequency was significantly different than 'Pre peak' with $p=0.02$, one-way ANOVA with Tukey's multiple comparisons correction, N=7 mice). Second, the number of neurons responding to the original best frequency decreased (Day 5: -38.4±29.4% decrease, mean±s.d.; Max: -31.3±19.4% decrease). The maximum change in percent of responsive neurons relative to initial tuning at the paired frequency occurred after several days of pairing (4.9±3.5 days; mean±s.d.; n=1018 neurons initially; n=934 neurons on day of max response; N=7 mice). As in our past studies of the behavioral effects of pairing auditory stimuli with basal forebrain stimulation[35], we hypothesize that both the changes to the paired and original best frequencies are required together, in order to effectively reshape cortical tuning curves for improving sensory perception.

VNS activates cholinergic basal forebrain neurons projecting to auditory cortex

A major outstanding question regarding the utility of VNS across species is the mechanisms of action. Specifically, it remains unclear how and where VNS leads to either direct or indirect activation of different brain regions (including auditory cortex). We reasoned that central neuromodulation was involved, given the diverse set of clinical applications of VNS in human subjects[39–42], the slower rates for consistent perceptual improvement and cortical plasticity seen in mice [35,61] and the known anatomical projections from NTS[56,57]. However, many of the effects of VNS have been historically attributed to the titratable activation of the locus coeruleus and consequent central noradrenergic release[49,54,55,62]. The potential contribution of cholinergic modulation to VNS has been more controversial. Conventionally the cholinergic basal forebrain was thought to receive only indirect input from NTS via locus coeruleus[56,57]. While behavioral evidence links motor learning with the recruitment of cholinergic basal forebrain neurons via

359 VNS[50,63], there are differences in the functional organization of cholinergic inputs to various
360 cortical regions[30,64–67]. Thus, we next wanted to establish if the central cholinergic system might
361 contribute to the sensory perceptual improvements we observed with VNS.
362
363 We asked if basal forebrain cholinergic cells were functionally activated by VNS. To do this, we
364 performed fiber photometry of basal forebrain cholinergic neurons in untrained animals with VNS
365 cuffs. We injected ChAT-Cre mice with a Cre-dependent GCaMP6s in basal forebrain and
366 implanted a fiber above the injection site. VNS was applied every 10 seconds for 20 trials and
367 lasted 500 ms at 30Hz at 0.8-1.0 mA (**Fig. 5a**). Consistent with other results[50], we found 500 ms
368 of VNS was sufficient to induce prolonged activation of basal forebrain cholinergic neurons in a
369 subset of trials (**Fig. 5b,c**). The average activation of cholinergic cell bodies by VNS on individual
370 trials was negatively correlated with baseline fluorescence, such that trials with relatively high
371 baseline prior to VNS onset were more likely to have lower average activation (**Extended Data**
372 **Fig. 7a,b**, Pearson's R=-0.30, p=0.02).
373
374 Since VNS robustly activated cholinergic basal forebrain neurons, we wanted to better understand
375 the anatomical pathway contributing to this activation. Previous work has shown that NTS projects
376 to LC[56], which in turn projects to basal forebrain[57]. We wanted verify if cholinergic neurons of the
377 basal forebrain were primarily indirectly activated by VNS via NTS projections to the locus
378 coeruleus or whether there was another previously underexplored pathway. To do this, we
379 performed retrograde tracing studies from cholinergic neurons in basal forebrain using a Cre-
380 inducible, retrograde pseudotyped monosynaptic rabies virus[68,69]. We targeted cholinergic neurons
381 by injecting pAAV-TREtight-mTagBFP2-B19G and pAAV-syn-FLEX-splitTVA-EGFP-tTA in

382 the basal forebrain of ChAT-Cre mice (N=3) or a AAV1 EF1a-FLEX-GTB (N=3) followed by an
383 injection of SADΔG-mCherry two weeks later (**Fig. 5d**). We found mCherry expression in both
384 NTS and locus coeruleus, indicating that basal forebrain cholinergic neurons likely receive direct
385 input from both areas (**Fig. 5e**, **Extended Data Fig. 7c,d**). We verified this result by injecting a
386 Cre-dependent tdTomato with a retrograde promoter in basal forebrain of TH-Cre animals
387 (**Extended Data Fig 7e**). We again saw tdTomato expression in NTS (**Extended Data Fig. 7e**).
388 These anatomical studies show that cholinergic basal forebrain neurons receive input from TH+
389 neurons in both locus coeruleus and NTS (**Extended Data Fig. 7f**).
390
391 We next wanted to explore if VNS could activate basal forebrain cholinergic axons projecting to
392 auditory cortex. Previous studies found that VNS can activate cholinergic fibers in cortex[48,49], but
393 for much longer stimulation periods than used in our task (1-10 second periods of VNS). Thus, we
394 used two-photon imaging of cholinergic axon fibers in auditory cortex (**Fig. 5f**) to more
395 specifically monitor recruitment of cortically-projecting cholinergic inputs that might produce the
396 behavioral and neuronal effects of VNS tone pairing described above (VNS for 500 ms at 30 Hz
397 at 0.8 mA). ChAT-Cre mice were injected with Cre-dependent GCaMP6s in basal forebrain, a
398 window was implanted over auditory cortex and a VNS cuff was applied to the left vagus nerve
399 (N=6). VNS was applied for 500 ms at 30 Hz at 0.8-1.0 mA every 2.5-26.6 seconds. We found
400 that VNS strongly activated many cholinergic axon fibers in auditory cortex on a trial-by-trial basis
401 at various timescales with some trials reaching maximum activation during or immediate after
402 VNS offset and some persisting for several seconds (**Fig. 5g**). VNS activated cholinergic axons
403 across regions within auditory cortex and across animals (**Fig. 5h,i**). Interestingly, unlike with
404 activation of cholinergic cell bodies via VNS, there was no significant correlation between baseline

405 activity and VNS evoked activation (**Extended Data Fig. 7g**, Pearson's R=0.04, p=0.71). The
406 difference in trial-by-trial activation of axons and cell bodies could be due to differences in
407 experimental techniques (measurement of bulk activation vs activation of axon segments) and/or
408 due to the diversity of inputs and projection targets of subsets of cholinergic neurons[64,65].
409
410 We then asked if VNS-mediated task improvement required acetylcholine receptors in auditory
411 cortex acutely. To do this, after we infused either atropine (a muscarinic acetylcholine receptor
412 antagonist) or vehicle in auditory cortex 30 minutes prior to behavior after animals underwent 20
413 days of VNS pairing (**Fig. 5j**). We then applied VNS in the same manner as described previously
414 (block-wise for 50 trials on/off, 500ms centered around center and non-center frequencies).
415 Blocking activation of local acetylcholine receptors increased the error rate at the frequencies
416 ±0.25 octaves from center (**Fig. 5k,l**, at ±0.25: atropine: orange, 91.0±24.5%, mean±s.d.; vehicle:
417 gray, 63.3±26.4%, mean±s.d., N=5, p=0.03, Student's one-tailed paired t-test). Therefore, VNS
418 applied at levels that induce behavioral improvements activates auditory cortical projecting
419 cholinergic neurons in basal forebrain and acetylcholine in auditory cortex impacts behavior
420 acutely.
421
422 **Optogenetic manipulation of the central cholinergic system and VNS**
423 In the final set of experiments, given the activation of cholinergic fibers in auditory cortex, we
424 asked how cholinergic modulation related to long-term VNS pairing in behaving animals. Since
425 areas of cortex receive input from distinct subsets of cholinergic neurons[64,65], we aimed to target
426 only the auditory cortical-projecting cholinergic neurons. For projection-specific opsin expression,
427 we bilaterally injected a retrograde, Cre-dependent channelrhodopsin-2 (ChR2) virus in auditory

428 cortex and implanted optic fibers above basal forebrain in eight ChAT-Cre animals trained on the
429 2AFC task (**Fig. 6a, Extended Data Fig. 8a**). After 9+ days in stage three, instead of VNS pairing
430 (as these animals were not cuffed), we optogenetically stimulated auditory cortical-projecting
431 cholinergic neurons in the same manner as VNS: 500 ms duration, 30 Hz pulse rate, centered
432 around the 250 ms tone during training blocks two and four. Control animals were trained in the
433 same manner, did not have significantly different baseline behavior (**Extended Data Fig. 8b,c,**)
434 and underwent the same pairing protocol as optogenetic stimulation animals but were injected with
435 a retrograde, Cre-dependent fluorophore virus (rg-FLEX-tdTomato), instead of channelrhodopsin-
436 2. Given that there was not a significant change in response rate before and after optogenetic
437 pairing (**Extended Data Fig. 8d**), no response trials were not included in comparisons for control
438 and ChR2-positive animals.
439
440 We found that optogenetic activation of cholinergic neurons during behavior led to similar
441 improvements in perceptual learning as with VNS pairing. The maximum change in 2AFC task
442 performance occurred several days after optogenetic pairing (**Fig. 6b**, N=8 mice). We compared
443 behavioral performance on the last three days optogenetic pairing ('Last 3') to three days of
444 baseline behavioral performance ('-2-0'). Maximum performance was significantly increased past
445 the level obtained just from days of stage three training in optogenetic stimulation animals (**Fig.**
446 **6c,d**, before optogenetic pairing: 71.1±3.1% correct over all center/non-center stimuli,
447 mean±s.e.m, last three days of pairing: 76.3±2.8% correct over all stimuli, N=8 mice, p=0.01,
448 Student's two-tailed paired t-test), but not control animals (**Fig. 6c,d**, pre: 74.8±2.5% correct,
449 mean±s.e.m, last three days of pairing: 75.6±3.0%, N=7, p=0.67, Student's two-tailed paired t-
450 test; difference in performance prior to optogenetic activation and during, experimental: 5.3±1.6%,

451 mean±s.e.m., N=8, control: 0.8±1.7%, N=7, p=0.04, Student's one-tailed unpaired t-test).
452 Performance gains occurred at specific non-center flanking frequencies as with VNS pairing,
453 specifically at ±0.5-1.5 octaves from center (**Fig. 6e,** behavior of individual animals shown in
454 **Extended Data Fig. 8e**). Optogenetic stimulation animals, but not control animals, had a
455 significant reduction in errors at the frequencies ±0.5 and ±1 octave from the center frequency, but
456 not ±0.25 octaves from center (**Fig. 6f,g,h**,**i**, control: difference at ±0.25: -1.4±2.2, difference at
457 ±0.5: -1.6±5.8%, difference at ±1: 3.8±5.9, mean±s.e.m.; optogenetic stimulation animals:
458 difference at ±0.25: -1.0±2.2%, difference at ±0.5: -12.0±4.8%, difference at ±1: -14.0±5.5%,
459 mean±s.e.m., for ±0.25: p=0.55, for ±0.5: p=0.09, for ±1: p=0.02, Student's one-tailed unpaired t-
460 test). Similar to VNS experimental animals, optogenetic activation of cholinergic basal forebrain
461 neurons did not acutely improve performance (**Fig. 6j**) or alter response rate (**Fig. 6k**). While
462 behavioral performance in block 1 did not show the significant improvement over time seen in
463 VNS experimental animals (**Fig. 6l**), the change in block 1 performance and overall performance
464 on the last three days of pairing relative to baseline were positively correlated (**Fig. 6m**, R=0.67,
465 p=0.06, N=8), consistent with VNS experimental animals.
466
467 While the decrease in error rates with optogenetic pairing occurred over a broader range of
468 stimulus frequencies than VNS pairing, the time course and specific reductions to off-center
469 flanking tones was a consistent feature of both pairing methods. These observations support the
470 hypothesis that the predominant effects of VNS pairing for this 2AFC task in mice is through
471 cholinergic recruitment. To test this hypothesis more directly, in **Figure 7** we show the results of
472 optogenetic suppression of cholinergic basal forebrain neurons during VNS pairing. In other
473 trained ChAT-Cre animals (N=6 mice also shown in **Fig. 1**), we bilaterally injected a Cre-

474 dependent inhibitory opsin (archaerhodopsin) in the basal forebrain, implanted optic fibers
475 bilaterally over basal forebrain (**Extended Data Fig. 9a**), and implanted a cuff electrode on the
476 left vagus nerve (**Fig. 7a**). We verified successful cuff implantation in six animals by looking for
477 both low impedance and reliable reduction in heart rate in response to VNS (**Extended Data Fig.**
478 **9b,c,d**). After 9+ days of stage three training, we began VNS pairing as before, i.e., performing
479 VNS on each training day during blocks two and four. During VNS pairing blocks, we
480 concurrently optogenetically suppressed ChAT+ basal forebrain neurons continuously for 500
481 msec starting 125 ms before tone onset. Given that there was not a significant change in response
482 rate before and after optogenetic pairing (**Extended Data Fig. 9e**), no response trials were not
483 included in comparisons for control and ChR2-positive animals. Optogenetic suppression of basal
484 forebrain cholinergic neurons completely prevented behavioral gains from VNS pairing in overall
485 performance (**Fig. 7b,c**, N=6 mice, before VNS and optogenetic suppression: 62.2±2.3% correct
486 over all center/non-center stimuli, day 18-20 of VNS and optogenetic suppression: 62.7±2.3%
487 correct over all stimuli, p=0.79, Student's two-tailed paired t-test) and compared to performance
488 gains seen in experimental animals (**Fig. 7d**, p=0.01, Student's two-tailed unpaired t-test).
489 Inhibition of cholinergic basal forebrain neurons during VNS also prevented VNS-mediated
490 improvements at frequencies ±0.25 and ±0.5 octaves from center (**Fig. 7e-g**, individual animals
491 shown in **Extended Data Fig. 9f**). No long-term changes were induced in these animals, as
492 performance on block one remained similar to baseline even after 18-20 days of VNS when
493 cholinergic activity was suppressed (**Fig. 7h,i**). Collectively our results highlight the importance
494 of the central cholinergic modulatory system for enhancements of perceptual learning via VNS.

495 **Discussion**

496 Although the central nervous system is highly plastic, there are limitations on the extent of changes
497 induced by different experiences or mechanisms. For the auditory 2AFC task we used here,
498 animals made the most errors within half an octave of the 'lick left' reference tone; VNS pairing
499 could reduce error rates and sharpen behavioral performance, albeit not completely. Some limits
500 in terms of plasticity and behavioral improvement are set by the physical properties of the sensory
501 epithelium. In the visual domain, this includes retinal photoreceptor density and single-photon
502 sensitivity[70,71]; for the auditory system, the ability to resolve different frequencies is constrained
503 by the biophysics of the cochlear membrane and hair cell dynamics[58,59]. These properties are likely
504 to provide hard bounds on perceptual resolution and are difficult to overcome by alternative
505 mechanisms for potential plasticity.

506

507 Other limitations, however, might be due to other factors such as motivational state, behavioral
508 engagement, and/or the understanding of task rules and variables. These other factors likely reflect
509 the activation (or lack thereof) of central modulatory systems including the cholinergic basal
510 forebrain[31,72,73]. Indeed, here we found that bidirectional regulation of cholinergic modulation
511 could affect 2AFC task performance, with activation of cholinergic neurons enhancing task
512 performance, whereas suppressing cholinergic neuron activity blocked the effects of VNS.
513 Similarly, we and others have previously shown that engagement in similar auditory[29–31,67] or
514 visual[27] tasks activates neurons of the cholinergic basal forebrain, that cholinergic modulation is
515 important for task performance[28,31], and that artificially enhancing cholinergic modulation (via
516 pharmacology or electrical/optogenetic stimulation) can boost task performance past the levels
517 achieved purely by behavioral training[24,28,31,34,35]. It remains unclear why the cholinergic basal

518 forebrain is not normally fully engaged during task performance. As the effects of VNS on task
519 performance were weakest for the best-performing animals, it is possible that the degree of
520 cholinergic activation is a major predictor of individual sensory processing abilities and perceptual
521 learning rates.
522
523 The vagus nerve is remarkably complex, connecting to with several peripheral organs to provide
524 a multiplexed input to the brainstem NTS[74]. In turn, the NTS sends projections to several regions
525 important for central neuromodulation, including the oxytocin system of the hypothalamus[75], the
526 noradrenergic locus coeruleus[56,57,75], and the cholinergic basal forebrain[64–66]. Potentially any or all
527 of these systems might be activated by VNS, although little is known how patterns of vagal
528 activation (either naturally occurring or via VNS) lead to similar or differential recruitment of
529 these diverse modulatory systems. The specific parameters used for VNS (e.g., stimulation rate or
530 intensity) might also lead to variability in terms of which types of vagus nerve fibers[76] and/or
531 downstream systems are reliably activated. We used here a consensus VNS parameter set found to
532 generally be effective across a number of different outcome measures and species[43,47–50], but there
533 could be other stimulation regimes or longer-term dynamics that might shift the net effects of VNS.
534 There may also be species-specificity in terms of central consequences of VNS. While aspects of
535 the neuroanatomical organization of the vagus and NTS seem largely conserved, the thickness and
536 composition of the vagus nerve bundle is considerably different across species, which would result
537 in different subsets of fibers being activated by electrical stimulation[77,78].
538
539 Despite this complexity, it appeared that VNS as used here in mice largely resulted in cholinergic
540 modulation of auditory cortex. Although NTS projects to locus coeruleus[56] and locus coeruleus

541 projects to basal forebrain[57], our anatomical tracing studies also revealed direct projections from
542 both the locus coeruleus and NTS to the basal forebrain, indicating that the cholinergic system
543 might be a major point of convergence for vagal inputs from the brainstem to affect cortical
544 function and behavior. Previous studies have shown that enhancement of perceptual learning and
545 behavioral performance with cholinergic modulation can be surprisingly slow, taking days to
546 weeks to emerge[24,61]. This is similar to the gradual improvements in 2AFC performance we
547 observed here with VNS pairing. In contrast, the effects of locus coeruleus pairing can be much
548 more rapid, but possibly at the expense of initial performance[61], and over-activation of the locus
549 coeruleus can cause behavioral arrest[79]. Previous work investigating how autonomous system can
550 activate central brain areas showed that activation of the autonomous system can cause anxiety-
551 like behaviors potentially via activation of the noradrenergic system[80]. This might account for why
552 we observed essentially no effects of VNS stimulation during or immediately after paired blocks,
553 but instead that the results of VNS pairing required days to be observed across animals. The
554 relatively slow expression of changes after VNS pairing might reflect a sleep-dependent process
555 requiring days for consolidation, and/or plasticity within neuromodulatory areas such as the basal
556 forebrain[29,30] or locus coeruleus[61] than then impact enhanced functionality only after reaching
557 some threshold level of modification. Additionally, if these systems are somewhat in opposition
558 or require temporally precise coordination[63,81], especially in terms of their short-term effects, it is
559 possible that combined stimulation of multiple modulatory centers leads to no net improvement in
560 the moment. Our work provides evidence that the sustained activation of the autonomous system
561 over many days can reverse the initial impact of activation from producing anxiety-like behaviors[80]
562 to mediating lasting perceptual improvements.
563

564 Neuroprosthetic devices can provide successful treatments for a wide range of debilitating
565 conditions, and perhaps could be adopted for use in augmenting performance outside of clinical
566 care. Some types of devices are implanted centrally, such as deep brain stimulation electrodes,
567 temporal lobe electrodes for regulating seizures, or motor cortex implants in cases of tetraplegia.
568 The invasive nature of central implants limits their utility to only the most severe conditions. In
569 contrast, more human subjects have received neuroprosthetic implants for peripheral nerve
570 stimulation; e.g., cochlear implants have been used in over 500,000 people and are largely
571 successful in terms of hearing restoration. Vagus nerve cuffs have been used in over 100,000
572 human subjects, mainly for treatment of epilepsy as well as other conditions[40]. A new generation
573 of less-invasive or non-invasive peripheral nerve stimulators targeting the hypoglossal nerve or
574 the auricular branch of the vagus nerve may be promising in terms of efficacy, although much
575 more work is required to validate these devices and determine optimal stimulation regimes[82]. Our
576 data suggest that some outcomes of successful VNS might take days, weeks, or even longer to be
577 revealed, and our results provide a potential mechanistic basis by which VNS can enhance auditory
578 perceptual learning.

579 **Methods**

580 **Animals**

581 All procedures were approved under an NYU Langone Institutional Animal Care and Use
582 Committee protocol. Male and female mice aged 6-20 weeks old were used in all experiments
583 (**Fig. 1**: N=38, 25 male, 13 female; **Fig. 2**: N=17, 12 male, 5 female; **Fig. 3**: N=17, 12 male, 5
584 female; **Fig. 4**: N=13, 4 male, 9 female; **Fig. 5**. N=14, 7 male, 7 female; **Fig. 6**: N=15, 7 male, 8
585 female; Fig. 7: N=6, 6 male). Genotypes used were wild-type C57BL/6J (The Jackson Laboratory,
586 Stock No: 000664), ChAT-Cre (The Jackson Laboratory, Stock No: 028861), and TH-Cre (The
587 Jackson Laboratory, Stock No: 008601). All mice had a C57BL/6J background. Mice were housed
588 in a temperature and humidity controlled room maintained on a 12 hour light/dark cycle. Animals
589 used in behavior were given 1 mL water/day. If their weight dropped below 80% of original, they
590 were given *ad libitum* water until weight returned to ≥80% original value.

591

592 **2AFC Behavioral Training**

593 Behavioral events (lick detection, auditory stimulus delivery, water reward delivery) were
594 monitored and controlled by custom MATLAB programs interfacing with an RZ6 auditory digital
595 signal processor (Tucker-Davis Technologies) via RPvdsEx software (Tucker-Davis
596 Technologies). Licks were detected using capacitance sensors (SparkFun, Part number:
597 AT42QT1011) and water was delivered using solenoids (The Lee Company, Part number:
598 LHDA0581215H). Animals were restrained using custom headposts (Ponoko).

599 Behavioral training on the auditory 2AFC task began after 7+ days of water restriction.
600 Training started with habituation to head-fixation with water delivered to the mouse while it sat in
601 a plexiglass tube. This was followed by lick port sampling sessions, in which the animal could

602 receive water by alternating licking between the two ports with a minimum of 3 seconds between
603 possible rewards. Mice typically learned to alternate ports while licking for 2-4 μL water droplets
604 in 2-4 sessions. Once animals reliably licked to receive water from lick ports, stage 1 training was
605 begun (i.e., animals were trained to lick left for the center frequency and lick right for one non-
606 center frequency). The center frequency was chosen to be either 11.3, 13.4, or 16 kHz (each animal
607 had a single consistent center frequency pseudo-randomly selected from those three values). Non-
608 center frequencies were set per animal to be ±0.25, ±0.5, ±1.0, and ±1.5 octaves from the selected
609 center frequency. In stage 1, the only non-center frequency was either +1.5 octaves or -1.5 octaves
610 from center (and whether higher or lower frequency was also pseudo-randomly assigned per
611 animal).

612 In stage 1, while an animal's performance remained <80% correct, they were rewarded
613 with water regardless of behavior choice on 15% of trials to help promote consistent licking during
614 training. Once performance reached ≥80% correct for three consecutive days in stage 1, animals
615 moved to stage 2 in which the other non-center frequency (either ± 1.5 octaves away) was added.
616 After three days in stage 2, animals moved to stage 3 regardless of performance (in which all other
617 non-center stimuli ±0.25, ±0.5, and ±1.0, octaves from the center frequency were also presented
618 and rewarded for right-side licking).

619 On each trial, a 250 ms tone was presented and animals had to classify the tone as the center
620 frequency (green) or any other frequency (shades of gray). Stimuli were presented at 70 dB SPL
621 in a pseudorandom order, such that the likelihood of center:non-center was 1:1 (with frequency
622 uniformly chosen from the non-center distribution on non-center trials). After a 250 ms delay,
623 animals had to lick left to report the stimulus as 'center' and had to lick right to report the stimulus
624 as 'non-center'. If the animal did not respond during the 2.5 seconds of the response epoch, the

625 trial was classified as a 'no response' trial (which were excluded from analysis except where
626 otherwise noted). If the lick response was correct, a small water reward (2-4 μL) was delivered to
627 the corresponding lick port. Inter-trial intervals were 3±0.5 seconds (mean±s.d.) on trials with a
628 correct response and 6±0.5 seconds (mean±s.d.) on trials with an incorrect response or without a
629 response. Animals were not punished for licking outside of the response epoch. Animals generally
630 performed between 350-500 trials/day.
631
632 **Vagus nerve stimulation in mice**
633 The custom cuff electrode design was adapted for mice from a previous cuff electrode designed
634 for rats[43,44]. A bipolar stimulating peripheral nerve cuff electrode was custom built using micro-
635 renathane tubing (Braintree Scientific, Part number: MRE-040), coated platinum iridium wire
636 (Medwire, Part number: 10IR9/49T), and gold pins (Mouser Electronics, Part number: 575-
637 100140). The tubing was used as the base for the portion of the cuff that interacts with the nerve.
638 It was cut in 1.0-1.5 mm segments, with an interior diameter of 0.025 inches to allow for nerve
639 swelling after implantation. Two platinum iridium wires with the coating removed were glued
640 (Dentsply Sirona, Triad gel) to the interior of the tubing about 0.5 mm apart. Gold pins were
641 soldered to the end of the wires opposite the tubing. The coating on the wire was only removed for
642 small portions at both ends to limit non-coated contact only to the gold pins and within the interior
643 circumference of the tubing. Wires were 2.5-3.0 cm in length in order to span from the skull to the
644 position of the cervical vagus. Non-absorbable silk suture string (Braintree Scientific, Part number:
645 SUT-S 104) was added to each side of the cuff opening to improve cuff handling and manipulation
646 during implantation. Viable cuff electrodes were determined by an impedance reading between 1-
647 10 kΩ at 1 kHz when submerged in saline (Peak Instruments LCR45).

648 Impedance measurements were taken each day of stimulation (Peak Instruments LCR45,
649 Frequency: 1kHz). Measurements of breathing rates, SpO_2, and heart rates were collected using a
650 thigh sensor (MouseOx) in animals lightly anesthetized with 0.75-1.5% isoflurane during VNS.
651 The vagus nerve was stimulated using a high-current stimulus isolator (World Precision
652 Instruments A385) triggered by a digital signal processor (RZ6, Tucker-Davis Technologies). VNS
653 parameters were based on previous work[43,48–50]: 100 μs pulse width, 30 Hz stimulation rate, 0.5
654 second duration. Stimulation intensity was 0.6-0.8 mA, based on the magnitude of the effect on
655 vitals (VNS intensity was 0.8 mA for imaging studies of **Figs. 4,5**).

656 Surgeries were performed on mice aged 6-12 weeks. Mice were anesthetized using
657 isoflurane (1.0-2.5%) and positioned in a stereotaxic frame (Kopf, model 923-B). Body
658 temperature was maintained at 37°C with a heating pad and rectal temperature probe. For behavior
659 and imaging experiments, a custom headpost[31] was attached to the skull using dental cement
660 (C&B-metabond), after thorough cleaning using hydrogen peroxide. Following all surgical
661 procedures, animals were given a nutritionally-fortified water gel for recovery assistance (Clear
662 H_2O DietGel Recovery, Part number: 72-06-5022).

663 For cuff implantation, a magnetic retractor base plate (Fine Science Tools, Part number:
664 1800-03) was used instead of a stereotaxic frame to allow for more flexible positioning of the
665 animal. Mice were positioned semi-supine at a 45° angel on their right side. Hair on the chest was
666 removed with Nair from the sternum to the left shoulder. The surgical site was sterilized by
667 alternating 70% ethanol and betadine washes. A 1.5 cm incision was made 0.5-1.0 cm to the left
668 of the top of the sternum, then the submandibular gland was separated and retracted from
669 connective tissue. Using blunt forceps (Fine Science Tools, Part number: 11231-30), the left
670 sternocleidomastoid and omohyoid muscles were separated and retracted until the carotid sheath

671 was accessible. A sterilized cuff electrode was led subcutaneously from the left side of the scalp
672 incision, between the ear and eye, and down to the chest incision site. Once positioned, the cuff
673 end of the electrode was deposited near the carotid sheath and the gold pin leads remained exposed
674 on the head. Using sharp forceps (Fine Science Tools, Part number: 11251-30), a 4 mm stretch of
675 the cervical vagus nerve was isolated from surrounding nerves and vasculature without direct
676 contact with the nerve. The cuff electrode was positioned around the vagus nerve so the nerve was
677 not taut and the non-coated intra-cuff wires had even contact with the nerve. The cuff was knotted
678 closed with non-absorbable silk suture string and muscles were returned to their original positions.
679 Absorbable sutures (Ethicon, Part number: W1621T) were occasionally made on the muscles to
680 keep the cuff from lifting the nerve ventrally. The submandibular gland was repositioned and the
681 skin was sutured closed with absorbable sutures (Ethicon, Part number: VCP433). The sutures
682 were sterilized with betadine and then sealed with surgical glue (Meridian). The electrode cuff
683 leads were secured near the headpost using dental cement (C&B-metabond). The incision was
684 covered with 4% topical lidocaine (L.M.X. 4). Cuff electrode impedance (1 kHz) was recorded
685 immediately after surgery and maintained a similar measurement from before implantation.
686 Successful cuff implantation was verified using both impedance measurements and changes in
687 vitals readings as described above.

688 All VNS during behavior started after the animals reached stable performance after a
689 minimum of nine days from start of stage three. All animals in either the VNS or sham group
690 received 17-20 days of stimulation. On each day of stimulation, animals performed a total of 400
691 trials, with 100 trials (two blocks of 50 trials, blocks two and four) of behavior with VNS. All
692 auditory stimuli were stimulated to avoid the animal using solely VNS to identify specific stimuli.

693 VNS lasted 500 ms and was centered around the tone, i.e., it started 125ms prior to tone onset and
694 ended 125ms after tone offset. Stimulation days ended with 100 trials of unstimulated behavior.
695
696 **Two-photon calcium imaging**
697 Cranial window implantation over left auditory cortex was performed, as previously described[31].
698 For cell body imaging, 1.0 µL of diluted CaMKII.GCaMP6f (AAV1, diluted 1:3 with dPBS or
699 AAV9, diluted 1:10 with dPBS, Addgene number: 100834) was injected in three locations
700 throughout auditory cortex (1.5 mm from lambda, along lateral suture). For axon imaging, 1.0 µL
701 of pAAV.Syn.Flex.GCaMP6s.WPRE.SV40 (diluted 1:2 in dPBS; Addgene: 100845-AAV5; AP:
702 -0.5 mm, ML: -1.8 mm, DV: -4.5 mm from brain surface) was injected in basal forebrain of
703 heterozygous ChAT-Cre mice.
704 Two-photon fluorescence of GCaMP6f/s was excited at 900 nm using a mode locked
705 Ti:Sapphire laser (MaiTai, Spectra-Physics, Mountain View, CA) and detected in the green
706 channel. Imaging was performed on a multiphoton imaging system (Moveable Objective
707 Microscope, Sutter Instruments) equipped with a water immersion objective (20X, NA=0.95,
708 Olympus) and the emission path was shielded from external light contamination. Images were
709 collected using ScanImage (Vidrio). To image auditory cortex, the objective was tilted to an angle
710 of 50–60°. Awake animals were head-fixed under the microscope and the stimulus isolator was
711 connected to the VNS cuff. We imaged using one of two systems: either a microscope covering
712 approximately ~300 μm^2 regions with galvo-galvo scanning at ~4Hz (0.26 s/frame) or a
713 microscope covering approximately ~450 μm^2 regions with resonance scanning at ~30Hz (laser
714 power ≤40 mW).

For VNS pairing while imaging excitatory neurons, the speaker was ~10 cm away from the ear contralateral to the window. A consistent region of excitatory neurons in layer 2/3 of A1 (based on vasculature and relative orientation of neurons) was imaged over all days of pairing. For baseline imaging, pure tones (70 dB SPL, 4–64 kHz, 250 ms, 10 ms cosine on/off ramps, quarter-octave spacing, 10 trials for each frequency) were delivered in pseudo-random sequence every 5 seconds. During pairing, one frequency (chosen based on the initial tuning of the area) was played concurrently with VNS every 2.5 seconds for 5 minutes.

Collected data were processed using the Suite2p analysis pipeline[83]. Recorded frames were aligned using a non-rigid motion correction algorithm. Regions of interest (representing excitatory neurons or cholinergic axon segments) were segmented in a semi-automated manner using a Suite2p based classifier. Additional ROIs were manually drawn on an average image of all motion-corrected images. Calcium fluorescence was extracted from all ROIs. Semi-automated data analysis was performed using custom Matlab (MathWorks) software. For each ROI, we corrected for potential neuropil contamination as previously described[84]. The ΔF/F (%) was calculated as the average change in fluorescence during the stimulus epoch relative to the 750 ms immediately prior to stimulus onset: $\Delta F/F\ (\%)=((F_t-F_0)/F_0)*100$. ROIs were included in additional analysis if they had a significant response (both $p<0.05$ Student's two-tailed, paired t-test comparing activity during any stimulus and pre-stimulus epochs and had a mean ΔF/F equal to 5% or above for all trials with a particular frequency). Neurons were matched across sessions using the automated MATLAB algorithm ROIMatchPub (https://github.com/ransona/ROIMatchPub) with a matching criteria threshold of 0.4 (consistent with Seghal, et al., 2021) and manually verified (examples shown in **Extended Data Fig. 5**).

738 **Fiber photometry**

739 Heterozygous ChAT-Cre mice were bilaterally injected with 1.0 µL of
740 pAAV.Syn.Flex.GCaMP6s.WPRE.SV40 (diluted 1:2 in dPBS; Addgene: 100845-AAV5) in basal
741 forebrain (AP: -0.5 mm, ML: -1.8 mm, DV: -4.5 mm from brain surface). Animals were head-
742 posted and a 400 µm optical fiber (Thorlabs, Item# CFMC54L05) was implanted in the left
743 hemisphere slightly above the injection site at -4.3 D-V. Experiments were performed three to four
744 weeks after surgery. Photometry was performed using a custom-built rig (Falkner et al., 2016;
745 Carcea et al., 2019). A 400 Hz sinusoidal blue light (40-45 µW) from a 470 nm LED (Thorlabs,
746 Item# M470F1) connected to a LED driver (Thorlabs, Item# LEDD1B) was delivered via the
747 optical fiber to excite GCaMP6s. We also used a control 330 Hz light (10 µW) from a 405 nm
748 LED (Thorlabs, Item# M405FP1) connected to a second LED driver. Light travelled via 405 nm
749 and 469 nm excitation filters via a dichroic mirror to the brain. Emitted light traveled back through
750 the same optical fiber via dichroic mirror and 525 nm emission filter, passed through an adjustable
751 zooming lens (Thorlabs, Item# SM1NR05) and was detected by a femtowatt silicon photoreceiver
752 (Newport, Item# 2151). Recordings were performed using RX8 Multi-I/O Processor (Tucker-
753 Davis Technologies). The envelopes of the signals were extracted in real time using Synapse
754 software (Tucker-Davis Technologies). The analog readout was low-pass filtered at 10 Hz.
755 Additional analysis was performed using custom MATLAB (Mathworks) software.

756

757 **Circuit tracing**

758 For monosynaptic pseudotype tracing studies, 0.5 µL of a mix of pAAV-TREtight0mTag-BFP2-
759 B19G (diluted 1:20 in dPBS; Addgene: 100799-AAV1) and pAAV-syn-FLEX-splitTVA-EGFP-
760 tTA (diluted 1:200 in dPBS; Addgene: 100798-AAV1) was injected into basal forebrain (AP: -0.5

761 mm, ML: -1.8 mm, DV: -4.5 mm from brain surface) of ChAT-Cre mice. After one week, 0.25 µL
762 of EnvA G-Deleted Rabies-mCherry (diluted 1:5 in dPBS; Addgene: 32636) was injected in the
763 basal forebrain using the same coordinates. For mapping potential connectivity between basal
764 forebrain, locus coeruleus and nucleus tractus solitarius, 0.75 µL of rgAAV-FLEX-tdTomato
765 (diluted 1:3 in dPBS; Addgene number: 28306) was injected in TH-Cre mice in basal forebrain
766 (AP: -0.5 mm, ML: -1.8 mm, DV: -4.5 mm from brain surface) using either a Hamilton syringe (5
767 µL) or Nanoject (Drummond Scientific; Part number: 3-000-207).

768 Animals were deeply anaesthetized with isoflurane and then transcardially perfused with
769 phosphate buffered saline (1x PBS) followed by 4% paraformaldehyde (PFA) in PBS. Animals
770 injected for circuit tracing studies were perfused 3-6 weeks after viral injection. Animals injected
771 for optogenetics behavioral experiments were perfused after completion of behavioral training.
772 After at least 12 hours in 4% PFA, brains were either transferred to PBS for sectioning with a
773 vibratome or to a 30% sucrose-PBS solution for 24-48 hours to prepare for cryosectioning. For
774 cryosectioning, brains were embedded in Tissue-Plus™ O.C.T. Compound medium (Thermo
775 Fisher Scientific, Item# 23-730) and sectioned using a cryostat (Leica). All sections were cut at 50
776 µm.

777 For animals injected with monosynaptic pseudotyped rabies, brain sections were washed
778 with PBS (3x10 min at room temperature) and incubated for 2 hours at room temperature in
779 blocking solution containing 5% normal goat serum (Millipore Sigma, Item # G6767) in 1% Triton
780 X-100 (Millipore Sigma, Item #11332481001) dissolved in PBS. Brain slices containing basal
781 forebrain were incubated in primary antibody (1:500 dilution of 3% normal goat serum in 1%
782 Triton X100 dissolved in PBS of chicken anti-GFP IgY, Abcam catalog # ab13970 and rabbit anti-
783 mCherry IgG, Abcam catalog # ab167453) for 24-48 hours at 4°C. Afterwards, slices were washed

784 and incubated for 1–2 hours at room temperature in secondary antibody (1:500 dilution in PBS,
785 goat anti-chicken IgY Alexa Fluor 488, Thermo Fisher Scientific cat. # A11039 and goat anti-
786 Rabbit IgG (H+L) Cross-Absorbed Secondary Antibody, Alexa Fluor 555, Thermo Fisher
787 Scientific Part number # A21428). Brain slices containing locus coeruleus and NTS were
788 incubated in primary antibody (1:500 dilution of 3% normal goat serum in 1% Triton X100
789 dissolved in PBS, rabbit anti-mCherry IgG, Abcam catalog # ab167453) for 24-48 hours at 4°C.
790 Slices were washed and incubated for 1–2 hours at room temperature in secondary antibody (1:500
791 dilution, goat anti-Rabbit IgG (H+L) Cross-Absorbed Secondary Antibody, Alexa Fluor 555,
792 Thermo Fisher Scientific Part number # A21428). Finally, slides were washed and coverslipped
793 using VECTASHIELD Antifade Mounting Medium with DAPI (Vector Labs Part number#: H-
794 1200-10). For all other animals, brain sections were washed with PBS and mounted using
795 VECTASHIELD Antifade Mounting Medium with DAPI. Slides were imaged using a Carl Zeiss
796 LSM 700 confocal microscope with four solid-state lasers (405/444, 488, 555, 639 nm) with
797 appropriate filter sets and/or an Olympus AS-VSW whole slide scanner with an X-cite 120LED
798 Boost High-Power LED Illumination system.

799 Individual brain sections were aligned with the Allen Brain Mouse Atlas[85] using the
800 QuickNII system[86]. The QuickNII system uses manual annotation and semi-automatic spatial
801 registration to transform the reference atlas to match the anatomical landmarks in the
802 corresponding experimental images. We then focused our quantification analysis to specific brain
803 areas of interest – basal forebrain (AP: -0.5 mm), locus coeruleus (AP: -5.34) and solitary nucleus
804 (AP: -6.36). Using the brain region outlines generated by QuickNII, we manually counted the
805 number of cell bodies in each area. All labeled cells were marked in dots in shades of gray on the
806 reference image for the corresponding anatomical plane.

807

808 **Optogenetic stimulation or inhibition of basal forebrain cholinergic neurons**

809 To stimulate auditory cortical projecting cholinergic neurons, 1.0 µL of AAVrg.EF1a.
810 doublefloxed.hChR2(H134R).EYFP.WPRE-HGHpA (diluted 1:2 with dPBS; Addgene number:
811 20298) was injected into auditory cortex as described above in ChAT-Cre animals. For optogenetic
812 inhibition, 0.50 µL of AAV5.FLEX.ArchT.tdTomato (diluted 1:2 with dPBS; Addgene number:
813 28305) was injected in basal forebrain of ChAT-Cre animals using the coordinates described
814 above. In both cases, optic fibers were implanted 50 µm above basal forebrain and the animal was
815 head-posted. Optic fibers were custom made of glass fibers (200 µm core; Thorlabs FT200UMT)
816 fitted with zirconia LC connectors (Precision Fiber Products MM-FER2007C-2300), secured
817 using glue (Krazy Glue). All fibers used had at least an 80% efficiency prior to implantation.

818 For optogenetic stimulation during behavior, cholinergic basal forebrain neurons were
819 bilaterally stimulated in the same way as VNS pairing (500 ms centered around the tone at 30 Hz;
820 two blocks of 50 stimulation trials surrounded by unstimulated trials). For optogenetic inactivation
821 experiments, cholinergic basal forebrain neurons were bilaterally inhibited using a 500 ms pulse,
822 presented in conjunction with VNS pairing. Light (either blue or yellow) was delivered using a
823 driver (Thorlabs LEDD1B), fiber coupled LED (Thorlabs M470F3 or M565F3), a patch cable
824 (Thorlabs M129L01), and a bifurcated fiber bundle (Thorlabs BFYL2LF01) connected to the
825 fibers using a mating sleeve (Thorlabs ADAL1). Laser power was calibrated across days and
826 between 1-3 mW for all optogenetics experiments during behavior.

Author Contributions

K.A.M., J.K.S and R.C.F. designed the experiments. K.A.M, E.S.P, and J.K.S. performed the experiments. K.A.M. performed analysis. E.S.P., S.S.F., and S.O.V. provided technical assistance. N.Z.T., E.S.P., D.A.M., M.J.M., and R.C.F. designed and validated the VNS cuff electrode. K.A.M and R.C.F. wrote the manuscript.

Acknowledgments

We thank A. Agha, C.L. Ebbesen, E. Glennon, E. Kay-Rivest, R.A. Kolaric, K.I. Nagel, D.H. Sanes, D.M. Schneider, M.A. Svirsky, J.T. Roland, and S. Valtcheva for comments, discussions, and/or technical assistance. We thank the GENIE Program, Janelia Research Campus, and the Howard Hughes Medical Institute for provision of GCaMP6s and ScanImage. This work was funded by grants from the Defense Advanced Research Projects Agency (N66001-17-2-4010 to R.C.F., D.A.M., and M.J.M.), the National Institute on Deafness and Other Communication Disorders (DC012557 to R.C.F.), and the National Science Foundation (to K.A.M. and J.K.S.).

References

1. Fu, Y.-X. *et al.* Temporal Specificity in the Cortical Plasticity of Visual Space Representation. *Science (1979)* **296**, 1999–2003 (2002).
2. Gilbert, C. D., Li, W. & Piech, V. Perceptual learning and adult cortical plasticity. *J Physiol* **587**, 2743–2751 (2009).
3. Khan, A. G. *et al.* Distinct learning-induced changes in stimulus selectivity and interactions of GABAergic interneuron classes in visual cortex. *Nat Neurosci* **21**, 851–859 (2018).
4. Poort, J. *et al.* Learning Enhances Sensory and Multiple Non-sensory Representations in Primary Visual Cortex. *Neuron* **86**, 1478–1490 (2015).
5. Schoups, A., Vogels, R., Qian, N. & Orban, G. Practising orientation identification improves orientation coding in V1 neurons. *Nature* **412**, 549–553 (2001).
6. Yan, Y. *et al.* Perceptual training continuously refines neuronal population codes in primary visual cortex. *Nat Neurosci* **17**, 1380–1387 (2014).
7. Yao, H. & Dan, Y. Stimulus Timing-Dependent Plasticity in Cortical Processing of Orientation. *Neuron* **32**, 315–323 (2001).
8. Recanzone, G. H., Schreiner, C. E. & Merzenich, M. M. Plasticity in the frequency representation of primary auditory cortex following discrimination training in adult owl monkeys. *The Journal of Neuroscience* **13**, 87 LP – 103 (1993).
9. Polley, D. B., Steinberg, E. E. & Merzenich, M. M. Perceptual Learning Directs Auditory Cortical Map Reorganization through Top-Down Influences. *The Journal of Neuroscience* **26**, 4970 LP – 4982 (2006).
10. Karmarkar, U. R. & Buonomano, D. v. Temporal specificity of perceptual learning in an auditory discrimination task. *Learning and Memory* **10**, 141–147 (2003).
11. Edeline, J.-M., Pham, P. & Weinberger, N. M. Rapid development of learning-induced receptive field plasticity in the auditory cortex. *Behavioral Neuroscience* vol. 107 539–551 Preprint at https://doi.org/10.1037/0735-7044.107.4.539 (1993).
12. Bakin, J. S. & Weinberger, N. M. Classical conditioning induces CS-specific receptive field plasticity in the auditory cortex of the guinea pig. *Brain Res* **536**, 271–286 (1990).
13. Recanzone, G. H., Merzenich, M. M., Jenkins, W. M., Grajski, K. A. & Dinse, H. R. Topographic reorganization of the hand representation in cortical area 3b owl monkeys trained in a frequency-discrimination task. *J Neurophysiol* **67**, 1031–1056 (1992).
14. Feldman, D. E. & Brecht, M. Map Plasticity in Somatosensory Cortex. *Science (1979)* **310**, 810–815 (2005).
15. Wilson, D. A. & Stevenson, R. J. Olfactory perceptual learning: the critical role of memory in odor discrimination. *Neurosci Biobehav Rev* **27**, 307–328 (2003).
16. Karni, A. & Sagi, D. The time course of learning a visual skill. *Nature* **365**, 250–252 (1993).
17. van Kerkoerle, T., Marik, S. A., Meyer zum Alten Borgloh, S. & Gilbert, C. D. Axonal plasticity associated with perceptual learning in adult macaque primary visual cortex. *Proceedings of the National Academy of Sciences* **115**, 10464 LP – 10469 (2018).

18. Tsodyks, M. & Gilbert, C. Neural networks and perceptual learning. *Nature* **431**, 775–781 (2004).
19. Bao, S., Chang, E. F., Woods, J. & Merzenich, M. M. Temporal plasticity in the primary auditory cortex induced by operant perceptual learning. *Nat Neurosci* **7**, 974–981 (2004).
20. David, S. v, Fritz, J. B. & Shamma, S. A. Task reward structure shapes rapid receptive field plasticity in auditory cortex. *Proceedings of the National Academy of Sciences* **109**, 2144 LP – 2149 (2012).
21. Froemke, R. C. Plasticity of Cortical Excitatory-Inhibitory Balance. *Annu Rev Neurosci* **38**, 195–219 (2015).
22. Magee, J. C. & Grienberger, C. Synaptic Plasticity Forms and Functions. *Annu Rev Neurosci* **43**, 95–117 (2020).
23. Kilgard, M. P. & Merzenich, M. M. Cortical Map Reorganization Enabled by Nucleus Basalis Activity. *Science (1979)* **279**, 1714–1718 (1998).
24. Reed, A. *et al.* Cortical Map Plasticity Improves Learning but Is Not Necessary for Improved Performance. *Neuron* **70**, 121–131 (2011).
25. Edeline, J.-M., Hars, B., Maho, C. & Hennevin, E. Transient and prolonged facilitation of tone-evoked responses induced by basal forebrain stimulations in the rat auditory cortex. *Exp Brain Res* **97**, 373–386 (1994).
26. Bakin, J. S. & Weinberger, N. M. Induction of a physiological memory in the cerebral cortex by stimulation of the nucleus basalis. *Proceedings of the National Academy of Sciences* **93**, 11219 LP – 11224 (1996).
27. Goard, M. & Dan, Y. Basal forebrain activation enhances cortical coding of natural scenes. *Nat Neurosci* **12**, 1444–1449 (2009).
28. Pinto, L. *et al.* Fast modulation of visual perception by basal forebrain cholinergic neurons. *Nat Neurosci* **16**, 1857–1863 (2013).
29. Guo, W., Robert, B. & Polley, D. B. The Cholinergic Basal Forebrain Links Auditory Stimuli with Delayed Reinforcement to Support Learning. *Neuron* **103**, 1164-1177.e6 (2019).
30. Robert, B. *et al.* A functional topography within the cholinergic basal forebrain for encoding sensory cues and behavioral reinforcement outcomes. *Elife* **10**, e69514 (2021).
31. Kuchibhotla, K. V *et al.* Parallel processing by cortical inhibition enables context-dependent behavior. *Nat Neurosci* **20**, 62–71 (2017).
32. Letzkus, J. J. *et al.* A disinhibitory microcircuit for associative fear learning in the auditory cortex. *Nature* **480**, 331–335 (2011).
33. Poorthuis, R. B., Enke, L. & Letzkus, J. J. Cholinergic circuit modulation through differential recruitment of neocortical interneuron types during behaviour. *J Physiol* **592**, 4155–4164 (2014).
34. Thiel, C. M., Friston, K. J. & Dolan, R. J. Cholinergic Modulation of Experience-Dependent Plasticity in Human Auditory Cortex. *Neuron* **35**, 567–574 (2002).
35. Froemke, R. C. *et al.* Long-term modification of cortical synapses improves sensory perception. *Nat Neurosci* **16**, 79–88 (2013).
36. Wilson, D. A., Fletcher, M. L. & Sullivan, R. M. Acetylcholine and Olfactory Perceptual Learnin. *Learning and Memory* **11**, 28–34 (2004).

37. Hegedüs, P., Sviatkó, K., Király, B., Martínez-Bellver, S. & Hangya, B. Cholinergic activity reflects reward expectations and predicts behavioral responses. *iScience* **26**, 105814 (2023).
38. Hangya, B., Ranade, S. P., Lorenc, M. & Kepecs, A. Central Cholinergic Neurons Are Rapidly Recruited by Reinforcement Feedback. *Cell* **162**, 1155–1168 (2015).
39. Penry, J. K. & Dean, J. C. Prevention of Intractable Partial Seizures by Intermittent Vagal Stimulation in Humans: Preliminary Results. *Epilepsia* **31**, S40–S43 (1990).
40. Fisher, B., DesMarteau, J. A., Koontz, E. H., Wilks, S. J. & Melamed, S. E. Responsive Vagus Nerve Stimulation for Drug Resistant Epilepsy: A Review of New Features and Practical Guidance for Advanced Practice Providers. *Front Neurol* **11**, (2021).
41. O'Reardon, J. P., Cristancho, P. & Peshek, A. D. Vagus Nerve Stimulation (VNS) and Treatment of Depression: To the Brainstem and Beyond. *Psychiatry (Edgmont)* **3**, 54–63 (2006).
42. Meyers, E. C. *et al.* Vagus Nerve Stimulation Enhances Stable Plasticity and Generalization of Stroke Recovery. *Stroke* **49**, 710–717 (2018).
43. Engineer, N. D. *et al.* Reversing pathological neural activity using targeted plasticity. *Nature* **470**, 101–104 (2011).
44. Nichols, J. A. *et al.* Vagus nerve stimulation modulates cortical synchrony and excitability through the activation of muscarinic receptors. *Neuroscience* **189**, 207–214 (2011).
45. Lai, J. & David, S. v. Short-Term Effects of Vagus Nerve Stimulation on Learning and Evoked Activity in Auditory Cortex. *eNeuro* **8**, ENEURO.0522-20.2021 (2021).
46. Lockard, J. S., Congdon, W. C. & DuCharme, L. L. Feasibility and Safety of Vagal Stimulation In Monkey Model. *Epilepsia* **31**, S20–S26 (1990).
47. Mughrabi, I. T. *et al.* Development and characterization of a chronic implant mouse model for vagus nerve stimulation. *Elife* **10**, e61270 (2021).
48. Mridha, Z. *et al.* Graded recruitment of pupil-linked neuromodulation by parametric stimulation of the vagus nerve. *Nat Commun* **12**, 1539 (2021).
49. Collins, L., Boddington, L., Steffan, P. J. & McCormick, D. Vagus nerve stimulation induces widespread cortical and behavioral activation. *Current Biology* **31**, 2088-2098.e3 (2021).
50. Bowles, S. *et al.* Vagus nerve stimulation drives selective circuit modulation through cholinergic reinforcement. *Neuron* **110**, 2867-2885.e7 (2022).
51. Buell, E. P. *et al.* Vagus Nerve Stimulation Rate and Duration Determine whether Sensory Pairing Produces Neural Plasticity. *Neuroscience* **406**, 290–299 (2019).
52. Hays, S. A. *et al.* Vagus nerve stimulation during rehabilitative training enhances recovery of forelimb function after ischemic stroke in aged rats. *Neurobiol Aging* **43**, 111–118 (2016).
53. Hays, S. A. *et al.* Vagus nerve stimulation during rehabilitative training improves functional recovery after intracerebral hemorrhage. *Stroke* **45**, 3097–3100 (2014).
54. Groves, D. A., Bowman, E. M. & Brown, V. J. Recordings from the rat locus coeruleus during acute vagal nerve stimulation in the anaesthetised rat. *Neurosci Lett* **379**, 174–179 (2005).

55. Hulsey, D. R. *et al.* Parametric characterization of neural activity in the locus coeruleus in response to vagus nerve stimulation. *Exp Neurol* **289**, 21–30 (2017).
56. van Bockstaele, E. J., Peoples, J. & Telegan, P. Efferent projections of the nucleus of the solitary tract to peri-Locus coeruleus dendrites in rat brain: Evidence for a monosynaptic pathway. *Journal of Comparative Neurology* **412**, 410–428 (1999).
57. Schwarz, L. A. & Luo, L. Organization of the Locus Coeruleus-Norepinephrine System. *Current Biology* **25**, R1051–R1056 (2015).
58. King, J. *et al.* Rodent auditory perception: Critical band limitations and plasticity. *Neuroscience* **296**, 55–65 (2015).
59. Heffner, H. & Masterton, B. Hearing in Glires: Domestic rabbit, cotton rat, feral house mouse, and kangaroo rat. *J Acoust Soc Am* **68**, 1584–1599 (1980).
60. Klein, A. S., Dolensek, N., Weiand, C. & Gogolla, N. Fear balance is maintained by bodily feedback to the insular cortex in mice. *Science (1979)* **374**, 1010–1015 (2021).
61. Martins, A. R. O. & Froemke, R. C. Coordinated forms of noradrenergic plasticity in the locus coeruleus and primary auditory cortex. *Nat Neurosci* **18**, 1483–1492 (2015).
62. Yakunina, N., Kim, S. S. & Nam, E.-C. Optimization of Transcutaneous Vagus Nerve Stimulation Using Functional MRI. *Neuromodulation: Technology at the Neural Interface* **20**, 290–300 (2017).
63. Hulsey, D. R. *et al.* Reorganization of Motor Cortex by Vagus Nerve Stimulation Requires Cholinergic Innervation. *Brain Stimul* **9**, 174–181 (2016).
64. Do, J. P. *et al.* Cell type-specific long-range connections of basal forebrain circuit. *Elife* **5**, e13214 (2016).
65. Kim, J.-H. *et al.* Selectivity of Neuromodulatory Projections from the Basal Forebrain and Locus Ceruleus to Primary Sensory Cortices. *The Journal of Neuroscience* **36**, 5314 LP – 5327 (2016).
66. Gielow, M. R. & Zaborszky, L. The Input-Output Relationship of the Cholinergic Basal Forebrain. *Cell Rep* **18**, 1817–1830 (2017).
67. Laszlovszky, T. *et al.* Distinct synchronization, cortical coupling and behavioral function of two basal forebrain cholinergic neuron types. *Nat Neurosci* **23**, 992–1003 (2020).
68. Wickersham, I. R., Finke, S., Conzelmann, K.-K. & Callaway, E. M. Retrograde neuronal tracing with a deletion-mutant rabies virus. *Nat Methods* **4**, 47–49 (2007).
69. Liu, K. *et al.* Lhx6-positive GABA-releasing neurons of the zona incerta promote sleep. *Nature* **548**, 582–587 (2017).
70. Hecht, S., Shlaer, S. & Pirenne, M. H. ENERGY, QUANTA, AND VISION . *Journal of General Physiology* **25**, 819–840 (1942).
71. Baylor, D. A., Lamb, T. D. & Yau, K. W. Responses of retinal rods to single photons. *J Physiol* **288**, 613–634 (1979).
72. Reimer, J. *et al.* Pupil fluctuations track rapid changes in adrenergic and cholinergic activity in cortex. *Nat Commun* **7**, 13289 (2016).
73. McGinley, M. J. *et al.* Waking State: Rapid Variations Modulate Neural and Behavioral Responses. *Neuron* **87**, 1143–1161 (2015).
74. Prechtl, J. C. & Powley, T. L. The fiber composition of the abdominal vagus of the rat. *Anat Embryol (Berl)* **181**, 101–115 (1990).

75. Cunningham, J. T., Mifflin, S. W., Gould, G. G. & Frazer, A. Induction of c-Fos and ΔFosB Immunoreactivity in Rat Brain by Vagal Nerve Stimulation. *Neuropsychopharmacology* **33**, 1884–1895 (2008).
76. Mao, X., Chang, Y.-C., Zanos, S. & Lajoie, G. Rapidly Inferring Personalized Neurostimulation Parameters with Meta-Learning: A Case Study of Individualized Fiber Recruitment in Vagus Nerve Stimulation. *bioRxiv* (2022) doi:10.1101/2022.09.06.506839.
77. Settell, M. L. *et al.* Functional vagotopy in the cervical vagus nerve of the domestic pig: Implications for the study of vagus nerve stimulation. *J Neural Eng* **17**, (2020).
78. Chang, R. B., Strochlic, D. E., Williams, E. K., Umans, B. D. & Liberles, S. D. Vagal Sensory Neuron Subtypes that Differentially Control Breathing. *Cell* **161**, 622–633 (2015).
79. Carter, M. E. *et al.* Tuning arousal with optogenetic modulation of locus coeruleus neurons. *Nat Neurosci* **13**, 1526–1533 (2010).
80. Hsueh, B. *et al.* Cardiogenic control of affective behavioural state. *Nature* (2023) doi:10.1038/s41586-023-05748-8.
81. Hulsey, D. R., Shedd, C. M., Sarker, S. F., Kilgard, M. P. & Hays, S. A. Norepinephrine and serotonin are required for vagus nerve stimulation directed cortical plasticity. *Exp Neurol* 112975 (2019) doi:10.1016/j.expneurol.2019.112975.
82. Yap, J. Y. Y. *et al.* Critical Review of Transcutaneous Vagus Nerve Stimulation: Challenges for Translation to Clinical Practice . *Frontiers in Neuroscience* vol. 14 Preprint at https://www.frontiersin.org/article/10.3389/fnins.2020.00284 (2020).
83. Pachitariu, M. *et al.* Suite2p: beyond 10,000 neurons with standard two-photon microscopy. *bioRxiv* 61507 (2017) doi:10.1101/061507.
84. Kerlin, A. M., Andermann, M. L., Berezovskii, V. K. & Reid, R. C. Broadly Tuned Response Properties of Diverse Inhibitory Neuron Subtypes in Mouse Visual Cortex. *Neuron* **67**, 858–871 (2010).
85. Lein, E. S. *et al.* Genome-wide atlas of gene expression in the adult mouse brain. *Nature* **445**, 168–176 (2007).
86. Puchades, M. A., Csucs, G., Ledergerber, D., Leergaard, T. B. & Bjaalie, J. G. Spatial registration of serial microscopic brain images to three-dimensional reference atlases with the QuickNII tool. *PLoS One* **14**, 1–14 (2019).

1056 **Figure Legends**

1057 **Figure 1. 2AFC task for mouse auditory frequency discrimination. a**, Behavioral
1058 schematic showing trial structure. On each trial, a head-restrained and water-restricted
1059 mouse is presented with a pure tone of a single frequency for 0.25 seconds at 70 dB SPL.
1060 Mice were trained to classify tones as either the center frequency (green) or non-center
1061 (shades of gray, with dark gray indicating closest to the center tone frequency and light gray
1062 indicating furthest from the center) by licking left (for center) or right (for non-center) in a
1063 response epoch 0.25-2.5 seconds from tone presentation. If tones were classified correctly,
1064 reward was delivered on the corresponding lick port. Inter-trial interval (ITI), 2.5 to 7
1065 seconds. **b**, Set of auditory training stimuli. The center frequency (11.3-16.0 kHz, specified
1066 per animal) was rewarded if the animal licked left; non-center frequency (±0.25-1.5 octaves
1067 from center frequency) was rewarded if the animal licked right. A single non-center
1068 frequency either -1.5 or 1.5 octaves from center tone was used in stage 1, the other ±1.5
1069 octave frequency was added in stage 2, all other stimuli added in stage 3. **c**, Mean
1070 performance across all three stages for example wild-type male mouse. When performance
1071 reached ≥80% for three consecutive days in stage 1 (lightest blue), this animal was
1072 transitioned to stage 2 (middle blue) for three days before moving to stage 3. Error bars,
1073 binomial confidence interval. **d**, Performance for all animals relative to day 1 of stage 2
1074 (N=38 mice). Heat map, % correct performance for each stage of training. Gray, no data
1075 (ND) as animals were not trained on those days. **e**, Number of days in stage 1 for all animals
1076 (median 10 days, inter-quartile range 7-13 days. Open circles, wild-type females (N=5);
1077 filled circles, wild-type males (N=11); open squares, ChAT-Cre females (N=8); filled
1078 squares, ChAT-Cre males (N=14). **f**, Percent reported center (i.e., licked left) across all

1079 stimuli in on day one of stage 3 (dotted lines) and day of maximum performance (solid
1080 lines). Gray lines, individual mice. Colored circles, means (N=38). **g**, Stability of individual
1081 performance at end of stage 3 (before starting VNS). Mean overall performance was stable
1082 for final six days of stage three; final days 1-3 (performance: 70.5±1.3% correct,
1083 mean±s.e.m, N=38) compared to final days 4-6 (performance: 70.5±1.3%, p=0.998
1084 compared to final days 1-3, Student's two-tailed paired t-test). Individually, only 2/38
1085 animals showed a significant difference ($p<0.05$, Student's two-tailed paired t-test) on final
1086 days 1-3 vs final days 4-6 (bold lines), 36/38 animals had individually stable performance
1087 (thin lines). n.s., not significant. **h**, Error rate for each stimulus. Small circles, individual
1088 mice. Error rate was significantly higher at ±0.25 and 0.5 octaves (dark gray, ±0.25 octave
1089 error rate: 67.6±3.1%, mean±s.e.m; medium gray, ±0.5 octave error rate: 45.2±3.3%)
1090 compared to center (green, center tone error rate; 15.5± 2.1%, $p<10^{-5}$ compared to ±0.25-
1091 0.5, one-way ANOVA with Tukey's multiple comparisons correction). **, $p<0.001$.
1092

1093 **Figure 2. VNS during behavior improves perceptual discrimination over days. a**,
1094 Schematic of cuff electrode implantation on mouse left vagus nerve. **b**, Schematic of VNS
1095 pairing during behavior. VNS was performed in two blocks of 50 trials (blue, blocks 2 and
1096 4), interleaved between blocks of no stimulation (gray, blocks 1, 3 and 5). VNS parameters:
1097 500 ms duration, 30 Hz rate, 0.6-0.8 mA intensity, centered around the tone for that trial.
1098 During blocks of VNS, stimuli of all frequencies (center and non-center) were presented
1099 during behavior. **c**, VNS pairing during behavior gradually improved performance relative
1100 to baseline (days after VNS cuff implantation prior to start of VNS pairing) over days (N=7
1101 mice). **d**, Performance over all stimuli improves after VNS pairing, but not in sham control
1102 animals. Percent correct on final days of VNS pairing (Days 18-20) across all frequencies
1103 in experimental animals (blue, closed circles, 77.1±3.1%, mean±s.e.m., N=7) in comparison
1104 to the behavior three days prior to VNS (black, closed circles, 'Day -2-0', 65.4±3.8%,
1105 p=0.008, Student's two-tailed paired t-test). Percent correct on final days (Days 18-20)
1106 across all frequencies in sham control animals (blue open circles, 67.4±2.8%, mean±s.e.m.,
1107 N=10) in comparison to behavior three days prior to sham pairing onset (black open circles,
1108 68.5±2.5%, mean±s.e.m., N=10, p=0.65, Student's two-tailed paired t-test). **e**, Difference
1109 in performance on day 18-20 of VNS or sham pairing compared to three days prior to pairing
1110 onset in experimental animals (closed circles, 11.7±3.0%, mean±s.e.m., N=7) compared to
1111 sham control animals (open circles, -1.1±2.4%, mean±s.e.m., N=10, p=0.004, Student's
1112 one-tailed unpaired t-test). **f**, Percent reported center at each frequency relative to center son
1113 the three days prior to VNS onset (black, 'Days -2-0', gray lines are individual mice) and
1114 behavior on the final days of VNS pairing (blue, 'Days 18-20', light blue lines are individual
1115 animals, N=7 mice). **g**, Percent correct at center frequency significantly increased on final

days of VNS pairing (blue, Days 18-20, 84.9±5.0%, mean±s.e.m.) compared to three days prior to pairing onset (black, Days -2-0, 71.6±7.0%, mean±s.e.m., p=0.02, Student's two-tailed paired t-test). **h**, Average percent reported center at ±0.25 (dark gray) and ±0.5 (medium gray) octaves normalized by performance at center frequency gradually reduced over days of stimulation (shaded blue) in experimental animals (solid line, N=7), but not sham controls (dotted line, N=10). **i**, Percent reported center normalized by performance at center frequency at ±0.25 octave from center was reduced over days prior to VNS pairing onset (black, Days -2-0) compared to the final days of VNS pairing (blue, Days 18-20) in experimental animals (solid lines, closed circles, Days -2-0: 91.6±7.0%, Days 18-20: 67.2±8.1%, mean±s.e.m., p=0.04, Student's two-tailed paired t-test), but not sham controls (dotted lines, open circles, Days -2-0: 95.3±3.9%, Days 18-20: 87.2±4.7%, mean±s.e.m., p=0.13, Student's two-tailed paired t-test). **j**, Percent reported center normalized by performance at center frequency at ±0.5 octave was reduced over days prior to VNS pairing onset (black, Days -2-0) compared to the final days of VNS pairing (blue, Days 18-20) in experimental animals (solid lines, closed circles, Days -2-0: 78.8±7.1%, Days 18-20: 49.2±6.8%, mean±s.e.m., p=0.01, Student's two-tailed paired t-test), but not sham-implanted control animals (dotted lines, open circles, Days -2-0: 74.8±5.1%, Days 18-20: 75.9±6.4%, mean±s.e.m., p=0.81). **k**, Difference in normalized percent reported center at ±0.25 and ±0.5 octave frequencies from center for sham controls (open circles, difference at ±0.25: -8.1±4.9, difference at ±0.5: 1.1±4.6%, mean±s.e.m.) and experimental animals (closed circles, difference at ±0.25: -24.3.1±9.2%, difference at ±0.5: -29.6±8.6%, mean±s.e.m., for ±0.25: p=0.06, for ±0.5: p=0.002, Student's one-tailed unpaired t-test).

1139 **Figure 3. VNS induces long-lasting behavioral improvements. a**, Performance for all
1140 stimuli is stable across blocks 1-4 on final three days with VNS in experimental animals
1141 (closed circles, block 1: 79.5±3.2% correct, mean±s.e.m., no VNS, black; block 2:
1142 79.1±1.9%, VNS, blue; block 3: 77.6±3.4%, no VNS, black; block 4: 75.8±2.5%, VNS,
1143 blue; p=0.78, one-way ANOVA with Tukey's multiple comparisons correction; N=7) and
1144 control animals (open circles, block 1: 73.3±2.7% correct, mean±s.e.m., no VNS, black;
1145 block 2: 65.5±4.6%, VNS, blue; block 3: 70.9±3.5%, no VNS, black; block 4: 64.9±4.8%,
1146 VNS, blue; p=0.37, one-way ANOVA with Tukey's multiple comparisons correction;
1147 N=10). **b**, Difference in performance across blocks with and without VNS for experimental
1148 (closed circles, average difference: -1.1±1.3%, mean±s.e.m.) and control animals (open
1149 circles, average difference: -6.9±3.8%, p=0.23, Student's two-tailed unpaired t-test). **c**,
1150 Performance for all stimuli was stable across blocks 1-4 prior to any days of VNS (block 1:
1151 68.0±4.3% correct, mean±s.e.m., no VNS, black; block 2: 63.9±3.6%, VNS, blue; block 3:
1152 63.1±3.7%, no VNS, black; block 4: 63.7±3.4%, VNS, blue; p=0.78, one-way ANOVA
1153 with Tukey's multiple comparisons correction; N=7). **d**, Percent reported center at each
1154 frequency relative to center stimulus on final days of VNS pairing in blocks with VNS (blue,
1155 blocks 2 and 4, light blue lines are individual animals) or without (black, blocks 1 and 3,
1156 gray lines are individual animals) in experimental (solid lines) and control mice (dotted
1157 lines). **e**, Difference in performance across block types (with or without VNS) at each
1158 frequency relative to the center stimulus for experimental (solid line) and control animals
1159 (dotted line, p=0.28 for frequencies, p=0.11 for experimental group, two-way ANOVA with
1160 Tukey's multiple comparisons correction). **f**, Response rate is stable across block 1-4 on
1161 final three days with VNS pairing in experimental (closed circles, block 1: 97.1±2.0%

correct, mean±s.e.m., no VNS, black; block 2: 98.2±1.6%, VNS, blue; block 3: 95.0±3.0%, no VNS, black; block 4: 95.5±2.8%, VNS, blue; p=0.77, one-way ANOVA with Tukey's multiple comparisons correction; N=7) and sham animals (open circles, block 1: 96.7±1.6% correct, mean±s.e.m., no VNS, black; block 2: 91.9±3.8%, "VNS", blue; block 3: 93.9±2.1%, no VNS, black; block 4: 85.7±5.7%, "VNS", blue; p=0.20, one-way ANOVA with Tukey's multiple comparisons correction; N=10). **g**, Difference in response rate across blocks with and without VNS for experimental (closed circles, average difference: 0.9±1.1%, mean±s.e.m.) and control animals (open circles, average difference: -6.5±3.7%, p=0.13, Student's two-tailed unpaired t-test). **h**, Mean change in percent correct relative to the three baseline days for all stimuli in block one (i.e., 50 trials prior to receiving VNS during behavior that day, black) and all subsequent trials (including 100 trials with VNS, blue) in an example animal. **i**, Summary of change in percent correct for all stimuli in block one (N=7 mice). **j**, Performance in block one during baseline sessions prior to VNS onset (black, 'Days -2-0') compared to performance on final days of VNS pairing (blue, 'Days 18-20') in experimental (closed circle, solid lines, average performance (Days -2-0): 68.0±4.3%, mean±s.e.m., average performance (Days 18-20): 79.5±3.2%, p=0.03, Student's two-tailed paired t-test, N=7) and control animals (open circle, dotted lines, average performance (Days -2-0): 69.5±1.9%, mean±s.e.m., average performance (Days 18-20): 73.3±2.7%, p=0.17, Student's two-tailed paired t-test, N=10). **k**, Difference in performance in block 1 between the three days prior to VNS pairing onset (Days -2-0) and the final three days of VNS pairing (Days 18-20) in experimental (closed circles, average difference: 11.5±4.1%, mean±s.e.m.) and control animals (open circles, average difference: 3.8±2.6%, p=0.057, Student's one-tailed unpaired t-test). **l**, Correlation between change in

1185 performance in block one and all subsequent trials in experimental animals (closed circles,
1186 Pearson's R=0.89, p=0.008, N=7) and control animals (open circles, Pearson's R=0.57,
1187 p=0.09, N=10).

1188 **Figure 4. VNS enables long-term plasticity in excitatory neurons in auditory cortex. a**,
1189 Schematic of VNS-tone pairing while performing two photon imaging of excitatory neurons
1190 in auditory cortex. During VNS-tone pairing, VNS was for 500ms at 30Hz, centered around
1191 the 250ms tone of one frequency every 2.5s. Pairing was done every day for up to 20 days.
1192 Control animals also heard a tone of one frequency at the same rate without the coincident
1193 VNS. During unpaired, passive tone presentation, tones ranging from 4-64 kHz at 70 dB
1194 are presented for 250ms every 5-10s. Passive tone presentation was performed every 1-3
1195 days. **b**, Portion of imaging region with ROIs colored for the frequency eliciting the
1196 maximal response in example animal during two days of passive tone presentation (Day 0:
1197 prior to receiving any VNS-tone pairing; Day 3: after receiving three days of VNS-tone
1198 pairing). Initial best frequency ("Pre-peak", black, open arrow), pairing frequency ("P",
1199 blue, closed arrow) and frequency ± one octave from the paired frequency ("±1", gray, open
1200 arrow) represented for example animal on color bar. **c**, Example ROIs tracked across 5 days
1201 of passive tone presentation (top: subset of neurons tracked over time; bottom: spatial
1202 overlap of all neurons tracked across all sessions within consistent imaging area, different
1203 colors represent different days of imaging). **d**, Percentage of significantly responsive
1204 neurons over two time points (initial day of unpaired passive tone presentation and day 5 of
1205 VNS pairing) in control (dotted lines, open circles; initial day: 33.0±8.1% significantly
1206 responsive to any frequency, mean±s.d, day 5: 21.5±10.6% responsive, N=4 mice,
1207 n=192±35.8 neurons per animal) and experimental animals (solid lines, closed circles;
1208 initial day: 30.2±10.7% significantly responsive to any frequency, mean±s.d, day 5:
1209 30.0±7.9% responsive, N=7 mice, n=145.3±20.5 neurons per animals, mean±s.d., p=0.96
1210 for experimental animals, p=0.20 for sham animals, Student's paired t-test, p=0.11 for

1211 difference across time points for experimental and sham animals, Student's unpaired t-test).
1212 **e**, Example neuron during initial passive tone presentation, after 5 days of VNS-tone pairing
1213 and after 12 days of VNS-tone pairing for select frequencies. The paired tone was 16 kHz
1214 (seen in blue) for this animal. Mean response for each frequency is represented in black and
1215 individual trials are shown in gray. **f**, Passive tuning curves across all frequencies for
1216 example neuron prior to first VNS pairing (lightest gray), +15 minutes post first VNS
1217 pairing (light gray), 5 days of VNS pairing (medium gray), and after 12 days of pairing
1218 (dark gray). 'VNS', paired tone was 16 kHz for this animal. '+1', tone one octave from
1219 paired tone. 'Pre', initial best frequency pre-peak across the population. **g**, Percentage of
1220 neurons responsive to 4 to 64 kHz prior to VNS pairing (lightest gray), 3 days of VNS
1221 pairing (light gray), 5 days of VNS pairing (medium gray) and after 9 days of pairing (dark
1222 gray) in example animal. The paired tone was 22.7 kHz for this animal. **h**, Change in percent
1223 responsive 15 minutes after initial VNS-tone pairing relative to initial responses at the
1224 frequency with the maximum initial response (Pre-peak; open circle; -31.4±29.9%;
1225 mean±s.d.), paired frequency (blue; 4.4±75.7%; mean±s.d.) and frequency one octave away
1226 from the paired frequency (gray; 59.3±164.1%; mean±s.d., N=9 mice, n=1303 neurons,
1227 144.8±33.2 neurons per animal, mean±s.d.; p=0.21; one-way ANOVA with Tukey's
1228 multiple comparisons correction). Example animal from **g** highlighted in dark gray. **i**,
1229 Change in percent responsive 2 hours after initial VNS-tone pairing relative to initial
1230 responses at the frequency with the maximum initial response (Pre peak; open circle; -
1231 9.0±52.9%; mean±s.d.), paired frequency (blue; 14.1±110.0%; mean±s.d.) and frequency
1232 one octave away from the paired frequency (gray; 64.8±119.5%; mean±s.d., N=9 mice,
1233 n=1303 neurons, 144.8±33.2 neurons per animal, mean±s.d.; p=0.29; one-way ANOVA

with Tukey's multiple comparisons correction). Example animal from **g** highlighted in dark gray. **j**, Change in percent responsive at day 5 of pairing relative to initial responses for at the frequency with the maximum initial response ('Pre peak', black), paired frequency (blue), and frequency one octave away from the paired frequency (±1, gray) for experimental (paired: 113.3±132.2%, mean±s.d.; Pre peak: -38.4±29.4%; Freq ±1: 57.9±133.4%; N=7 mice, n=953 total neurons, 136.1±16.5 neurons per animal; p=0.055; one-way ANOVA with Tukey's multiple comparisons correction) and sham animals (paired: -28.0±68.5%, mean±s.d.; Pre peak: -50.4±19.0%; Freq ±1: 38.2±188.9%; N=4 mice, n=737 neurons total, 184.3±37.1 neurons per animal; p=0.56; one-way ANOVA with Tukey's multiple comparisons correction). Example animal from **g** highlighted in dark gray. **k**, Distribution of days to maximum response at paired frequency (4.9±3.5 days; mean±s.d.; N=7 mice). Gray circle is animal represented in **g. l**, Change in percent responsive at day of maximum population response to paired frequency relative to initial response at with the maximum initial response ('Pre peak', black), paired frequency (blue), and frequency one octave away from the paired frequency (±1, gray) for experimental (paired: 263.2±295.2%, mean±s.d.; Pre peak: -31.3±19.4%; Freq ±1: 22.3±105.1%; N=7 mice, n=934 neurons total, 133.4±15.5 neurons per animal; p=0.02; one-way ANOVA with Tukey's multiple comparisons correction) and sham animals (paired: 82.0±33.6%, mean±s.d.; Pre peak: -28.7±30.1%; Freq ±1: 100.1±163.8%; mean±s.d., N=4 mice, n=750 neurons total, 187.5±43.8 neurons per animal; p=0.19; one-way ANOVA with Tukey's multiple comparisons correction). Day of maximum population response was determined for individual animals in **k**. Example animal from **g** highlighted in dark gray.

1257 **Figure 5. Stimulating the vagus nerve activates auditory-cortical projecting**
1258 **cholinergic basal forebrain. a**, Schematic of fiber photometry from cholinergic basal
1259 forebrain neurons. **b**, ΔF/F from all VNS applications for one example animal. VNS was
1260 applied for 500 ms at 30 Hz at 1.0 mA every 10 seconds. **c**, Average ΔF/F for all VNS trials
1261 across animals with mean baseline ΔF/F less than zero (N=3 mice; n=36 trials). **d**,
1262 Schematic for mapping inputs to cholinergic basal forebrain neurons using retrograde, Cre-
1263 dependent, pseudotyped monosynaptic rabies. Example image of injection area in basal
1264 forebrain, corresponding section from the Allen Brain Atlas, and location of GFP labeled
1265 neurons. The regions of interest are highlighted in red. Each animal is represented in a
1266 distinct shade of gray (N=3). **e**, Location of mCherry labeled neurons in section containing
1267 NTS labeled by dots in shades of gray. Regions of interest are highlighted in red. Each
1268 animal is represented in a distinct shade of gray (N=6). **f**, Schematic of imaging of basal
1269 forebrain cholinergic axons in auditory cortex. Trace of fluorescent activity is from one
1270 example animal from one example region. VNS applied for 500 ms at 30 Hz at 0.8 mA
1271 every 20 s. **g**, VNS triggered average from one example region. Example animal is the same
1272 shown in **f**. **h**, Distribution of time to max ΔF/F relative to VNS onset across all VNS
1273 applications in all regions in all animals (N=6 mice, 16.5±6.3 regions per animal, mean±s.d.,
1274 n=270 trials). VNS was applied for 500ms at 30Hz at 0.8-1.0 mA every 2.5-26.7s. **i**,
1275 Average ΔF/F for 1s baseline prior to VNS onset and 1s following VNS onset (shaded in
1276 light blue in **l**, N=6, VNS: 128.7±36.4% ΔF/F, mean±s.e.m., p=0.02, Student's two-tailed
1277 paired t-test). **j**, Schematic for local injection of either atropine (orange) or vehicle (gray,
1278 control) in auditory cortex after 20 days of VNS pairing during behavior. After local
1279 injection, VNS was applied during behavior in the same manner as described in **Figure 2**.

1280 **k**, Percent reported center across all frequencies for either atropine (individual animals
1281 represented in light orange, mean in darker orange) or vehicle (individual animals
1282 represented in light gray, mean in darker gray). **l**, Normalized percent reported center for
1283 atropine or vehicle at frequencies ±0.25 (atropine: orange, 91.0±24.5%, mean±s.d.; vehicle:
1284 gray, 63.3±26.4%, mean±s.d., N=5, p=0.03, Student's one-tailed paired t-test) and ±0.5
1285 from center (atropine: orange, 69.5±48.0%, mean±s.d.; vehicle: gray, 57.0±20.2%,
1286 mean±s.d., N=5, p=0.21, Student's one-tailed paired t-test).
1287

1288 **Figure 6. Activating auditory cortical projecting cholinergic basal forebrain neurons**
1289 **improves perceptual performance. a**, Schematic of optogenetic activation of auditory
1290 cortical projecting cholinergic BF neurons during behavior. Auditory cortical projecting
1291 cholinergic BF neurons were targeted using a retrograde Cre-dependent channelrhodopsin
1292 injected into auditory cortex of ChAT-Cre mice. ChAT+ BF activation was applied in the
1293 same blockwise fashion as previously described for 500 ms at 30 Hz centered around the
1294 tones. **b**, Optogenetic activation of ChAT+ BF neurons during behavior gradually improved
1295 performance over days (N=8 mice). **c**, Performance over all stimuli improves after
1296 optogenetic pairing in experimental animals (closed circles), but not control animals (open
1297 circles). Percent correct on the final three days of channelrhodopsin pairing for each animal
1298 all frequencies (light blue; experimental mean: 76.3±2.8%, mean±s.e.m., N=8; control
1299 mean: 75.6±3.0%, N=7) in comparison to the behavior three days prior to pairing onset
1300 (black; experimental mean: 71.1±3.1%, p=0.01, Student's two-tailed paired t-test, N=8;
1301 control mean: 74.8±2.5%, p=0.67, Student's two-tailed paired t-test, N=7). **d**, Difference in
1302 performance on the last three days of channelrhodopsin pairing relative to three days prior
1303 to pairing onset for experimental (closed circles, 5.3±1.6%, mean±s.e.m., N=8) or control
1304 animals (open circles, 0.8±1.7%, N=7, p=0.04, Student's one-tailed unpaired t-test). **e**,
1305 Percent reported center at each frequency relative to center stimulus on the three days prior
1306 to optogenetic pairing onset (black) and behavior on the last three days of channelrhodopsin
1307 pairing (light blue) in experimental (solid lines, N=8) and control animals (dotted lines,
1308 N=7). **f**, Percent reported center normalized by performance at the center frequency at ±0.25
1309 octave frequency from center was not significantly reduced over days prior to
1310 channelrhodopsin pairing onset (black, Days -2-0) compared to the final days of

1311 channelrhodopsin pairing (blue, 'Last 3') in experimental animals (solid lines, closed
1312 circles, Days -2-0: 84.6±6.4%, Last 3: 83.6±6.9%, mean±s.e.m., p=0.67, Student's two-
1313 tailed paired t-test) or control animals (dotted lines, open circles, Days -2-0: 87.5±4.8%,
1314 Last 3: 86.2±5.0%, mean±s.e.m., p=0.56, Student's two-tailed paired t-test). **g**, Percent
1315 reported center normalized by performance at the center frequency at ±0.5 octave frequency
1316 from center was significantly reduced over days prior to optogenetic pairing onset (black,
1317 Days -2-0) compared to the final days of channelrhodopsin pairing (blue, 'Last 3') in
1318 experimental animals (solid lines, closed circles, Days -2-0: 70.9±7.9%, Last 3: 58.9±9.7%,
1319 mean±s.e.m., p=0.04, Student's two-tailed paired t-test), but not control animals (dotted
1320 lines, open circles, Days -2-0: 62.9±7.2%, Last 3: 61.3±5.3%, mean±s.e.m., p=0.80,
1321 Student's two-tailed paired t-test). **h**, Percent reported center normalized by performance at
1322 the center frequency at ±1 octave frequency from center was not significantly reduced over
1323 days prior to channelrhodopsin pairing onset (black, Days -2-0) compared to the final days
1324 of channelrhodopsin pairing (blue, 'Last 3') in experimental animals (solid lines, closed
1325 circles, Days -2-0: 47.5±9.0%, Last 3: 33.5±6.8%, mean±s.e.m., p=0.04, Student's two-
1326 tailed paired t-test) or control animals (dotted lines, open circles, Days -2-0: 30.7±5.9%,
1327 Last 3: 34.4±10.2%, mean±s.e.m., p=0.55, Student's two-tailed paired t-test). **i**, Difference
1328 in normalized percent reported center at ±0.5 and ±1 octave frequencies from center for
1329 control animals (open circles, difference at ±0.5: -1.6±5.8, difference at ±1: 3.8±5.9%,
1330 mean±s.e.m.) and experimental animals (closed circles, difference at ±0.5: -12.0±4.8%,
1331 difference at ±1: -14.0±5.5%, mean±s.e.m., for ±0.5: p=0.09, for ±1: p=0.02, Student's one-
1332 tailed unpaired t-test). **j**, Performance for all stimuli is stable across blocks 1-4 on final three
1333 days with optogenetic stimulation in experimental animals (closed circles, block 1:

74.7±2.6% correct, mean±s.e.m., no ChR2+ pairing, black; block 2: 75.1±2.7%, ChR2+ pairing, blue; block 3: 75.2±3.5%, no ChR2+ pairing, black; block 4: 74.8±3.1%, ChR2+ pairing, blue; p=0.99, one-way ANOVA with Tukey's multiple comparisons correction; N=8). **k**, Response rate is stable across block 1-4 on final three days with optogenetic pairing in experimental animals (block 1: 92.3±3.7% correct, mean±s.e.m., no ChR2+ pairing, black; block 2: 92.2±4.1%, ChR2+ pairing, blue; block 3: 92.0±4.5%, no ChR2+ pairing, black; block 4: 92.3±4.5%, ChR2+ pairing, blue; p=0.99, one-way ANOVA with Tukey's multiple comparisons correction; N=8). **l**, Performance in block one during baseline sessions prior to optogenetic pairing onset (black, Days -2-0: 72.6±3.5%, mean±s.e.m.) compared to performance on final three days of channelrhodopsin pairing (blue, Last 3: 74.7±2.6%, p=0.50, Student's two-tailed paired t-test, N=8). **m**, Correlation between change in performance in block one and all subsequent trials (Pearson's R=0.67, p=0.06, N=8).

1347 **Figure 7. Inhibiting cholinergic basal forebrain neurons during VNS blunts VNS-**
1348 **mediated perceptual improvements. a**, Schematic of VNS and optogenetic inhibition of
1349 cholinergic BF neurons during behavior. VNS was applied in the same blockwise fashion
1350 as previously described. Cholinergic BF neurons were optogenetically inhibited using a
1351 Cre-dependent Archaerhodopsin and green light (565 nm) for the entire duration of VNS
1352 during behavior (500 ms). **b**, Optogenetic inhibition of ChAT+ BF neurons during VNS
1353 during behavior abolishes improved performance (N=6 mice). **c**, Performance did not
1354 improve after optogenetic inhibition during VNS. Percent correct on the final three days of
1355 optogenetic inhibition during VNS (Days 18-20; yellow; 62.7±2.3%, mean±s.e.m., N=6) in
1356 comparison to the behavior three days prior to VNS (black; 62.2±2.3%, p=0.79, Student's
1357 two-tailed paired t-test). **d**, Difference in performance on day 18-20 of VNS pairing relative
1358 to three days prior to pairing onset for animals receiving VNS with optogenetic inhibition
1359 of cholinergic basal forebrain neurons (yellow, 0.5±1.7%, mean±s.e.m., N=6) or without
1360 (blue, 11.7±3.0%, mean±s.e.m., N=7, p=0.01, Student's two-tailed unpaired t-test). **e**,
1361 Percent reported center at each frequency relative to center stimulus on the three days prior
1362 to start of optogenetic inhibition with VNS pairing onset (black) and the final three days of
1363 pairing (yellow, Days 18-20, N=6 mice). **f**, Percent reported center normalized by
1364 performance at the center frequency at ±0.25 and ±0.5 octave frequency from center was
1365 not significantly reduced over days prior to VNS pairing onset (black, Days -2-0 (±0.25):
1366 97.6±2.5%, Days -2-0 (±0.5): 84.3±6.3%, mean±s.e.m.) compared to the final days of VNS
1367 pairing (yellow, Days 18-20 (±0.25): 94.5±1.8%, Days 18-20 (±0.5): 79.8±6.5%,
1368 p(±0.25)=0.15, p(±0.5)=0.33, Student's two-tailed paired t-test). **g**, Difference in
1369 normalized percent reported center at ±0.25 and ±0.5 octave frequencies from center for

1370 animals with optogenetic inhibition of cholinergic basal forebrain neurons during VNS
1371 pairing (yellow, difference at ±0.25: -3.1±1.8%, difference at ±0.5: -4.5 ±4.2%,
1372 mean±s.e.m.) or without (blue, difference at ±0.25: -24.3±9.2%, difference at ±0.5: -29.6
1373 ±8.6%, mean±s.e.m., for ±0.25: p=0.04, for ±0.5: p=0.03, Student's one-tailed unpaired t-
1374 test). **h**, Performance in block one during baseline sessions prior to pairing onset (black,
1375 Days -2-0: 62.4±3.4%, mean±s.e.m.) compared to performance on final days of VNS and
1376 optogenetic inhibition of cholinergic basal forebrain neuron pairing (yellow, Days 18-20:
1377 65.8±3.4%, p=0.15, Student's two-tailed paired t-test, N=6). **i**, Correlation between change
1378 in performance in block one and all subsequent trials (Pearson's R=-0.26, p=0.63, N=6).

1379 **Extended Data Figure 1. Performance is stable and does not significantly improve**
1380 **after seven days in stage 3. a**, Lick rates relative to tone offset from one session in six fully
1381 trained example animals (shades of gray represent individual animals). **b**, Lick rates in the
1382 second after tone offset (2.6±0.84 licks/s, mean±s.d., N=6) are significantly higher than lick
1383 rates 2-3 seconds after tone offset (0.2±0.3 licks/s, p=0.0002, Student's two-tailed paired t-
1384 test, N=6). **c**, Change in performance across all frequencies throughout all days in stage 3
1385 relative to the performance on the first three days of stage 3 (N=38). **d**, Correlation between
1386 total days animals spend in stage three and peak performance in stage 3 (Pearson's R=0.31,
1387 p=0.06, N=38). **e**, Mean performance significantly improved across days (Days 0-2:
1388 64.7±1.0%; Days 6-8: 70.0±1.2%; Days max±1: 72.6±1.3%, mean±s.d.; p<0.00002 one-
1389 way ANOVA with Tukey's multiple comparisons correction, N=38 animals). **f**, Across-
1390 animal performance is variable on day 7 of stage three (69.0±8.0%, mean±s.d., N=38
1391 animals). **g**, Percent reported center at each frequency relative to center stimulus on days 0-
1392 2, days 6-8 and behavior on day of maximum performance in stage 3. **h**, Error rate at
1393 frequencies 0 (green; day 1-3: 18.7±2.3%, day 7-9: 18.3±2.0%, Max day ± 1 day:
1394 15.0±1.8%, mean±s.e.m.; p=0.36, one-way ANOVA with Tukey's multiple comparisons
1395 correction), ±0.25 (dark gray; day 1-3: 79.2±2.4%, day 7-9: 71.0± 2.7%, Max±1:
1396 73.0±2.5%, mean±s.e.m.; p=0.07, one-way ANOVA with Tukey's multiple comparisons
1397 correction) and ±0.5 (medium gray; day 1-3: 69.8±2.9 %, day 7-9: 56.2±2.7%, Max±1:
1398 53.6±2.9%, mean±s.e.m.; p=0.0002, one-way ANOVA with Tukey's multiple comparisons
1399 correction) from center over days 0-2 (open circles, white), 6-8 (open circles, gray), and
1400 max (± 1 day, closed circles) in stage 3.
1401

Extended Data Figure 2. Additional training did not continue to improve performance. a, Percent reported left for all days in stage 3 for animals trained for 21-48 days in stage 3 (36.3±12.4 days in stage 3, N=6). ND (gray) represents days with no data collection. **b**, Schematic for reward size modulation experiments performed in days following performance shown in **a**. After animals were fully trained and had stable performance, animals received rewards of double the volume for all frequencies for 12-13 additional days. **c**, Performance over all frequencies over days of altered reward size. **d**, Average percent reported center for the five days prior to increased reward size and last five days on increased reward size. **e**, Performance across the two reward sizes (smaller reward, more trials: open circle, larger reward, fewer trials: closed circle) at 0 (small reward: 78.9±4.1% correct, for large reward: 83.5±3.3%, mean±s.e.m; p=0.15, Student's two-tailed paired t-test), ±0.25 (small reward: 36.9±6.8% correct, large reward: 35.4±4.3%, mean± s.e.m.; p=0.67, Student's two-tailed paired t-test), and ±0.5 (small reward: 64.2±7.0% correct, large reward: 71.4±6.3%, mean± s.e.m.; p=0.08, Student's two-tailed paired t-test).

1418 **Extended Data Figure 3. VNS transiently alters heart rate in viable cuffs. a,** Impedance
1419 over days post-implantation from a representative animal (top) and all 7 wild-type mice
1420 used for VNS pairing behavioral experiments. Gray, individual animals; black, mean±s.d.
1421 every 10 days (N=7 mice). **b**, Cuff impedance is stable over time. Impedance reading on
1422 day 0 (day of cuff implantation) and the first measurement 30+ days after implantation (30-
1423 54 days) (Day 0 mean: 2.7±0.6 kΩ, day 30-54 mean: 2.3±1.6 kΩ, mean±s.d., N=7 mice,
1424 p=0.56, Student's two-tailed paired t-test). **c**, Description of vitals recordings. Sessions with
1425 and without VNS application were alternated. Between 10 and 20 VNS bouts occurred in
1426 each VNS session and lasted 500 ms at 0.1 Hz. Stimulation intensity was consistent within
1427 a session but was systematically changed throughout the day (ranging from 0.2 to 1.4 mA).
1428 The following data is from sessions with VNS (0.8-1.0 mA) compared to the baseline
1429 sessions immediately prior or following. **d**, Distribution of heart rate was not significantly
1430 different during VNS or baseline sessions in two animals with cuff impedances >100MΩ
1431 (Sham 1, cuff impedance: 100MΩ, p=0.66, Mann Whitney U two-sided test; Sham 2, cuff
1432 impedance: 120MΩ, p=0.48, Mann Whitney U two-sided test). **e**, Raw heart rate from
1433 example animal with viable cuff. VNS was applied at 0.1 Hz and lasted 500 ms. **f**,
1434 Distribution of heart rates in VNS and baseline sessions for ten animals with potentially
1435 viable cuffs (VNS significantly reduced heart rate in 7/10 animals; Animal 1, cuff
1436 impedance: 0.2 kΩ, $p<10^{-5}$, Mann Whitney U two-sided test; Animal 2, cuff impedance: 3.4
1437 kΩ, $p<10^{-5}$; Animal 3, cuff impedance: 3.0 kΩ, $p<10^{-5}$; Animal 4, cuff impedance: 0.1 kΩ,
1438 p=0.03; Animal 5, cuff impedance: 2.8 kΩ, $p<10^{-5}$; Animal 6, cuff impedance: 3.9 kΩ, $p<10^{-}$
1439 ^{5}; Animal 7, cuff impedance: 3.9 kΩ, $p<10^{-5}$; Sham 3, cuff impedance: 2.1 kΩ, p>0.05;
1440 Sham 4, cuff impedance: 1.9 kΩ, p>0.05; Sham 5, cuff impedance: 3.6 kΩ, p>0.05).

1441 **Extended Data Figure 4. Experimental and control animals have consistent behavior**
1442 **prior to VNS pairing. a**, Distribution of days in stage one for sham control (gray, 13.9±6.0
1443 days, mean±s.d., N=10) and experimental animals (black, 10.4±4.4 days, mean±s.d., N=7,
1444 p=0.16, Mann Whitney U two-sided test). **b**, Distribution of days spent in stage 3 prior to
1445 VNS pairing for sham control (gray, 17.5±6.8 days, mean±s.d., N=10) and experimental
1446 animals (black, 21.1±10.6 days, mean±s.d., N=7, p=0.40, Mann Whitney U two-sided test).
1447 **c**, Distribution of response rate in stage 3 for sham control (gray, 96.1±5.0%, mean±s.d.,
1448 N=10) and experimental animals (black, 91.3±7.5%, mean±s.d., N=7, p=0.14, Mann
1449 Whitney U two-sided test). **d**, Distribution of peak performance in stage 3 for sham control
1450 (gray, 73.4±6.1%, mean±s.d., N=10) and experimental animals (black, 68.7±10.0%,
1451 mean±s.d., N=7, p=0.36, Mann Whitney U two-sided test). **e**, Percent reported center for
1452 sham (dotted lines, N=10) and experimental animals (solid lines, N=7, p=0.20, two-way
1453 ANOVA with Tukey's multiple comparisons correction). **f**, Performance is not affected by
1454 VNS cuff implantation in experimental (-1.8±1.7%, mean±s.e.m., N=7, p=0.38, Student's
1455 two-tailed paired t-test) or sham animal (0.4±1.0%, mean±s.e.m., N=10, p=0.68, Student's
1456 two-tailed paired t-test; difference between sham and experimental: p=0.28, Student's two-
1457 tailed unpaired t-test).
1458

1459 **Extended Data Figure 5. Impact of VNS pairing on experimental and control animals.**
1460 **a**, Change in response rate for the three days prior to VNS onset and on days 18-20 of VNS
1461 pairing for sham (gray, -7.8±2.4% response rate, mean±s.e.m., N=10) and experimental
1462 animals (black, 4.5±2.1% response rate, mean±s.e.m., N=7, p=0.002, Student's two-tailed
1463 unpaired t-test). **b**, Response rate across frequencies for the three days prior to VNS onset
1464 (black) and on days 18-20 of VNS pairing (blue) for experimental animals (p=0.32 across
1465 frequencies, p<0.001 across days, ANOVA with Tukey's multiple comparisons correction).
1466 **c**, Percent correct on final days of VNS pairing (Days 18-20) across all frequencies in
1467 experimental animals (blue, closed circles, without: 80.4±2.4%, mean±s.e.m., with:
1468 77.1±3.1%, N=7) in comparison to the behavior three days prior to VNS (black, closed
1469 circles, 'Day -2-0', without: 71.6±3.5%, with: 65.4±3.8%) with (p=0.008, Student's paired
1470 t-test) and without no response trials (without: p=0.02, Student's paired t-test). **d**, Change
1471 in response rate for the three days prior to VNS onset and days 18-20 of VNS pairing across
1472 three groups of intensities used for control animals (p=0.4, one-way ANOVA with Tukey's
1473 multiple comparisons correction, N=10). **e**, Percent of trials reported as center for all
1474 animals used in VNS pairing experiments for the three days prior to VNS onset (black) and
1475 on days 18-20 of VNS pairing (blue) used in Figure 2 and 3 (Control: N=10, dotted lines;
1476 Experimental: N=7, solid lines).
1477

Extended Data Figure 6. Tracking neurons during two-photon imaging. a, Example ROIs in an example animal during unpaired passive tone presentation on days 0, 3, 6, 9 and 11 days of VNS pairing. Average Pearson's R correlation for 20x20 pixel area containing ROIs and surrounding area across all days. **b**, Average Pearson's R correlation for 20x20 pixel area containing ROIs and surrounding area across all days of passive tone presentation ("Imaging days") for all VNS pairing animals (N=7; Average R (animal 1): 0.59±0.15, mean±s.d.; Average R (animal 2): 0.67±0.12; Average R (animal 3): 0.69±0.08; Average R (animal 4): 0.52±0.18; Average R (animal 5): 0.69±0.13; Average R (animal 6): 0.61±0.15; Average R (animal 7): 0.57±0.19).

1487 **Extended Data Figure 7. Activation of basal forebrain cholinergic neurons by VNS. a**,
1488 Correlation between baseline activity of cholinergic cell bodies in 1.5s prior to VNS onset
1489 and average activity in 1.5s following VNS onset (Pearson's R=-0.30, p=0.02, N=3 mice,
1490 n=60 trials). **b**, Cholinergic cell body responses prior to or during VNS separated by
1491 baseline responses (higher than zero or lower than or equal to zero). Responses in 500ms
1492 after VNS were significantly higher in trials with low baseline (during VNS: 0.47±0.16%
1493 ΔF/F, p=0.006, Student's two-tailed t-test) but not during trials with high baseline (during
1494 VNS: -0.21±0.19% ΔF/F, p=0.26, Student's two-tailed t-test). **c**, Example basal forebrain
1495 and NTS section with alignment to corresponding output from QuickNII system of Allen
1496 Brain Atlas section with either basal forebrain or NTS circled in white. **d**, Schematic for
1497 mapping inputs to cholinergic basal forebrain neurons using retrograde, Cre-dependent,
1498 pseudotyped monosynaptic rabies. Location of mCherry labeled neurons in section
1499 containing LC labeled by dots in shades of gray. The region of interest is highlighted in red.
1500 Each animal is represented in a distinct shade of gray (N=5). **e**, Schematic of injection of
1501 retrograde Cre-dependent tdTomato into basal forebrain of TH-Cre mice. Location of
1502 tdTomato labeled neurons in section containing NTS labeled by dots in shades of gray. The
1503 region of interest is highlighted in red. Each animal is represented in a distinct shade of gray
1504 (N=4). **f**, Schematic of proposed anatomical connections between NTS, locus coeruleus
1505 and basal forebrain. **g**, Correlation between baseline cholinergic axon activity in 1s prior to
1506 VNS onset and average activity in the 1s following VNS onset (Pearson's R=0.04, p=0.71).
1507

1508 **Extended Data Fig. 8. Impact of stimulating auditory cortical projecting cholinergic**
1509 **neurons on individual animal performance. a**, Verification of fiber placement over basal
1510 forebrain in one example animal. Scale bar is 1200 μm. **b**, Distribution of peak performance
1511 prior to optogenetic pairing onset of control (open circles, 77.1±2.5% correct, mean±s.e.m.)
1512 and experimental animals ('ChR2', closed circles, 72.1±2.8% correct, mean ± s.e.m.,
1513 p=0.15, Mann Whitney U two-sided test). **c**, Percent of trials reported center for control
1514 (dotted lines, mean in blue, individual animals in gray, N=7) and experimental animals
1515 (solid lines, mean in blue, individual animals in gray, N=8). **d**, Difference in response rate
1516 in the three days prior to optogenetic or sham pairing and on the last three days of
1517 optogenetic or sham pairing in control (open circles, -0.28±7.5% change in response rate,
1518 mean±s.e.m, N=7) or experimental animals (closed circles, -1.7±1.8% change in response
1519 rate, mean±s.e.m., N=8, p=0.86, Student's two-tailed unpaired t-test). **e**, Percent of trials
1520 reported as center for 15 animals in **Figure 6** for the three days prior to optogenetic or sham
1521 pairing onset (black) and on the last three days with optogenetic or sham pairing (blue).
1522 Experimental animals are represented with solid lines and sham animals are represented
1523 with dotted lines.
1524
1525

1526 **Extended Data Figure 9. Impact of inhibiting cholinergic neurons in basal forebrain**
1527 **during VNS on individual animal performance. a**, Verification of fiber of fiber
1528 placement over basal forebrain in one example animal. Scale bar is 1200 µm. **e**, Percent of
1529 trials reported as center for 6 animals in **Fig. 7** for the three days prior to VNS onset (black)
1530 and days 18-20 of VNS stimulation (orange). **b,** Description of vitals recordings. Sessions
1531 with and without VNS application were alternated. Between 10 and 20 VNS bouts occurred
1532 in each VNS session and lasted 500 ms at 0.1 Hz. Stimulation intensity was consistent
1533 within a session but was systematically changed throughout the day (ranging from 0.2 to
1534 1.4 mA). The following data is from sessions with VNS (0.8-1.0 mA) compared to the
1535 baseline sessions immediately prior or following. **c**, Example baseline and VNS session
1536 from example animal. **d**, Distribution of heart rates in VNS (blue) and baseline (gray)
1537 sessions for six animals with potentially viable cuffs ($p<0.001$, Mann Whitney U two-sided
1538 test). **e**, Difference in response rate in the three days prior to VNS pairing and on day 18-20
1539 of VNS pairing with inhibition of cholinergic basal forebrain neurons (1.4±3.3% change in
1540 response rate, mean±s.e.m, N=6). **f**, Percent of trials reported as center for 6 animals in
1541 Figure 7 for the three days prior to optoinhibition during VNS pairing onset (black) and on
1542 the last three days with optoinhibition during VNS pairing (orange).

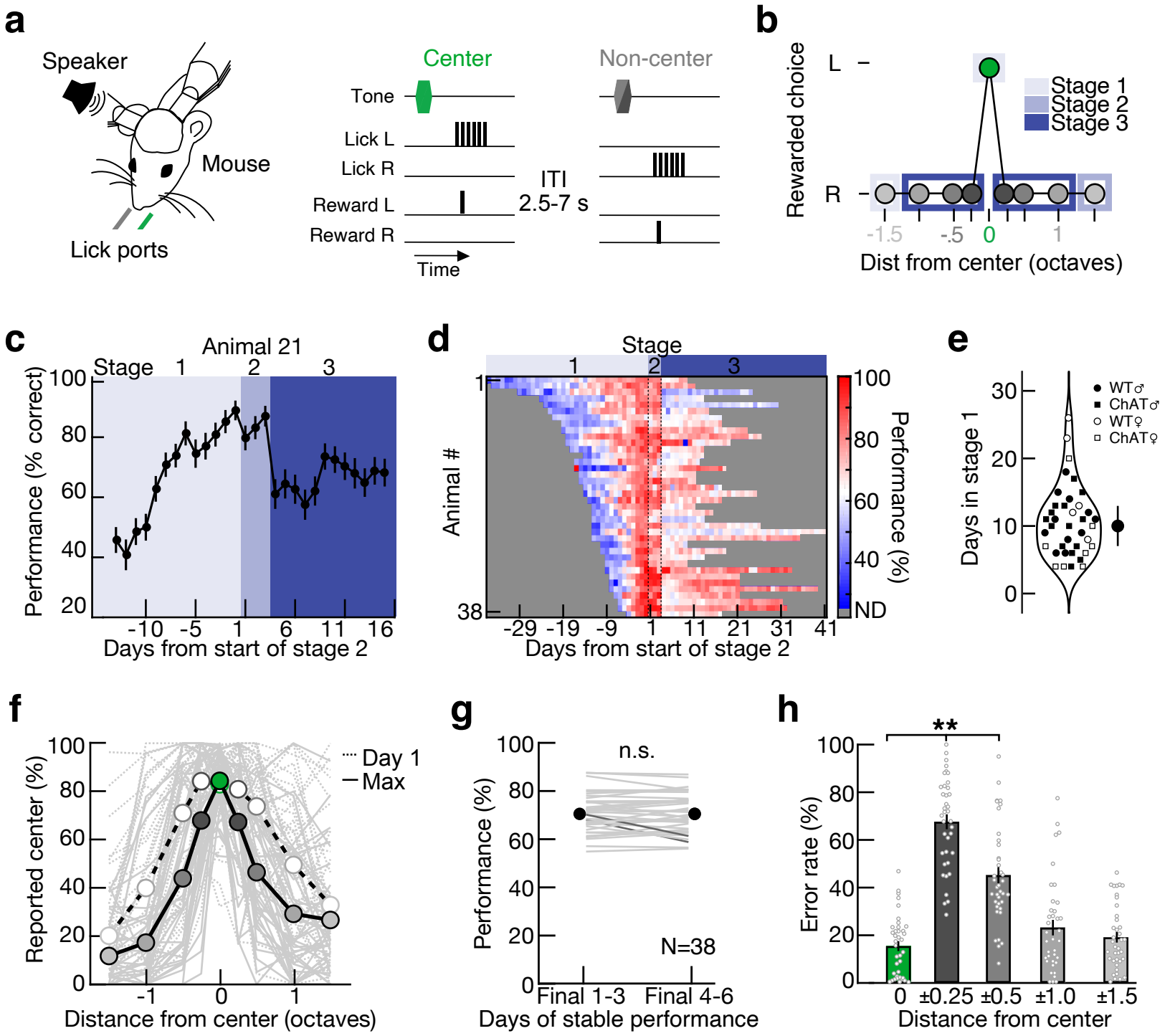
a
Speaker
Mouse
Lick ports
Center
Non-center
Tone
Lick L
Lick R
Reward L
Reward R
ITI
2.5-7 s
Time
b
Rewarded choice
L
R
Stage 1
Stage 2
Stage 3
-1.5
-.5
0
1
Dist from center (octaves)
c
Animal 21
Stage
1
2
3
Performance (% correct)
100
80
60
40
20
-10
-5
1
6
11
16
Days from start of stage 2
d
Stage
1
2
3
Animal #
1
38
-29
-19
-9
1
11
21
31
41
Days from start of stage 2
Performance (%)
100
80
60
40
ND
e
Days in stage 1
30
20
10
0
WT♂
ChAT♂
WT♀
ChAT♀
f
Reported center (%)
100
80
60
40
20
0
-1
0
1
Distance from center (octaves)
Day 1
Max
g
Performance (%)
100
80
60
40
20
0
n.s.
N=38
Final 1-3
Final 4-6
Days of stable performance
h
Error rate (%)
100
80
60
40
20
0
**
0
±0.25
±0.5
±1.0
±1.5
Distance from center

Figure 1

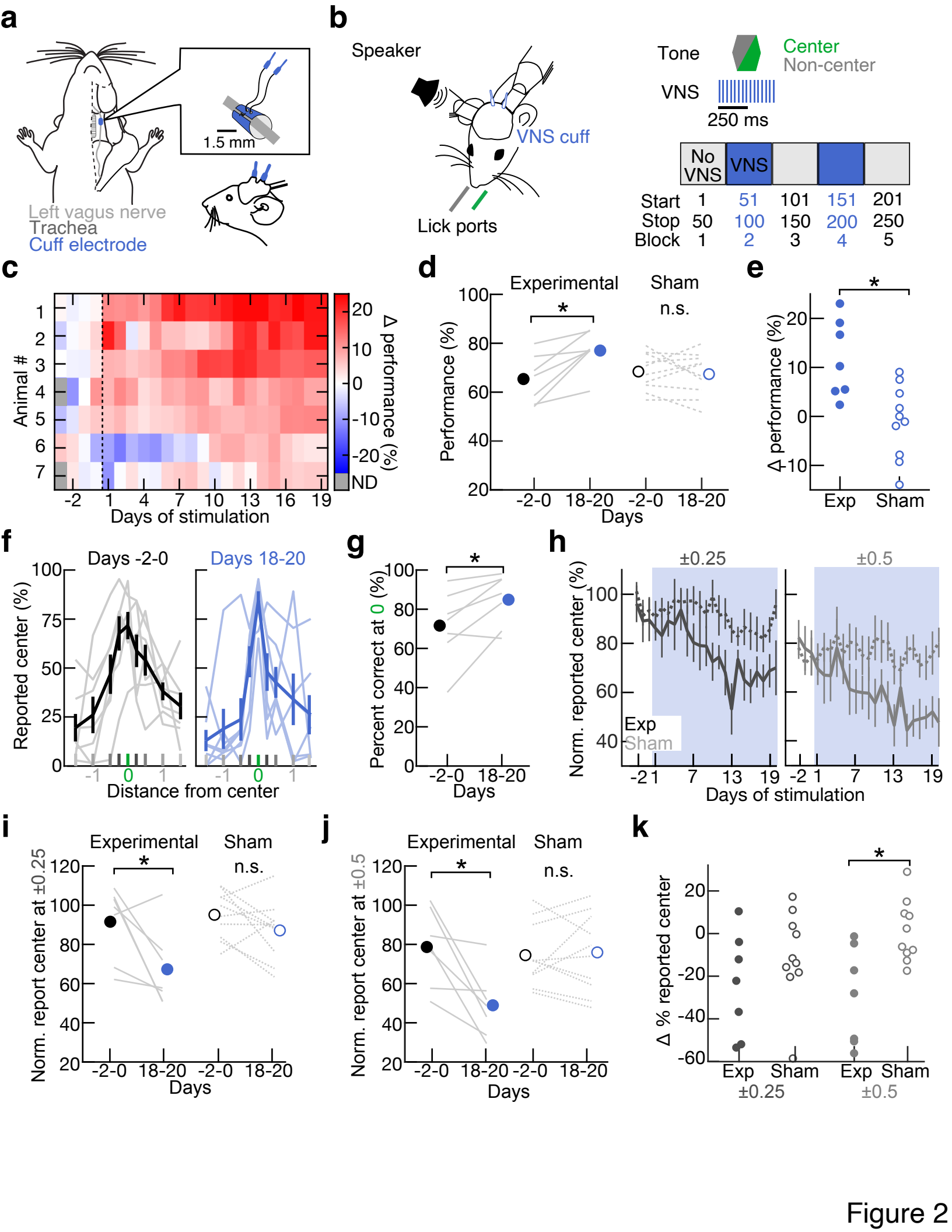
a
1.5 mm
Left vagus nerve
Trachea
Cuff electrode
b
Speaker
VNS cuff
Lick ports
Tone
Center
Non-center
VNS
250 ms
No VNS
VNS
Start 1 51 101 151 201
Stop 50 100 150 200 250
Block 1 2 3 4 5
c
Animal #
Days of stimulation
Δ performance (%)
ND
d
Experimental
Sham
n.s.
Performance (%)
Days
e
Δ performance (%)
Exp
Sham
f
Days -2-0
Days 18-20
Reported center (%)
Distance from center
g
Percent correct at 0 (%)
Days
h
±0.25
±0.5
Norm. reported center (%)
Exp
Sham
Days of stimulation
i
Experimental
Sham
n.s.
Norm. report center at ±0.25
Days
j
Experimental
Sham
n.s.
Norm. report center at ±0.5
Days
k
Δ % reported center
Exp
Sham
±0.25
±0.5

Figure 2

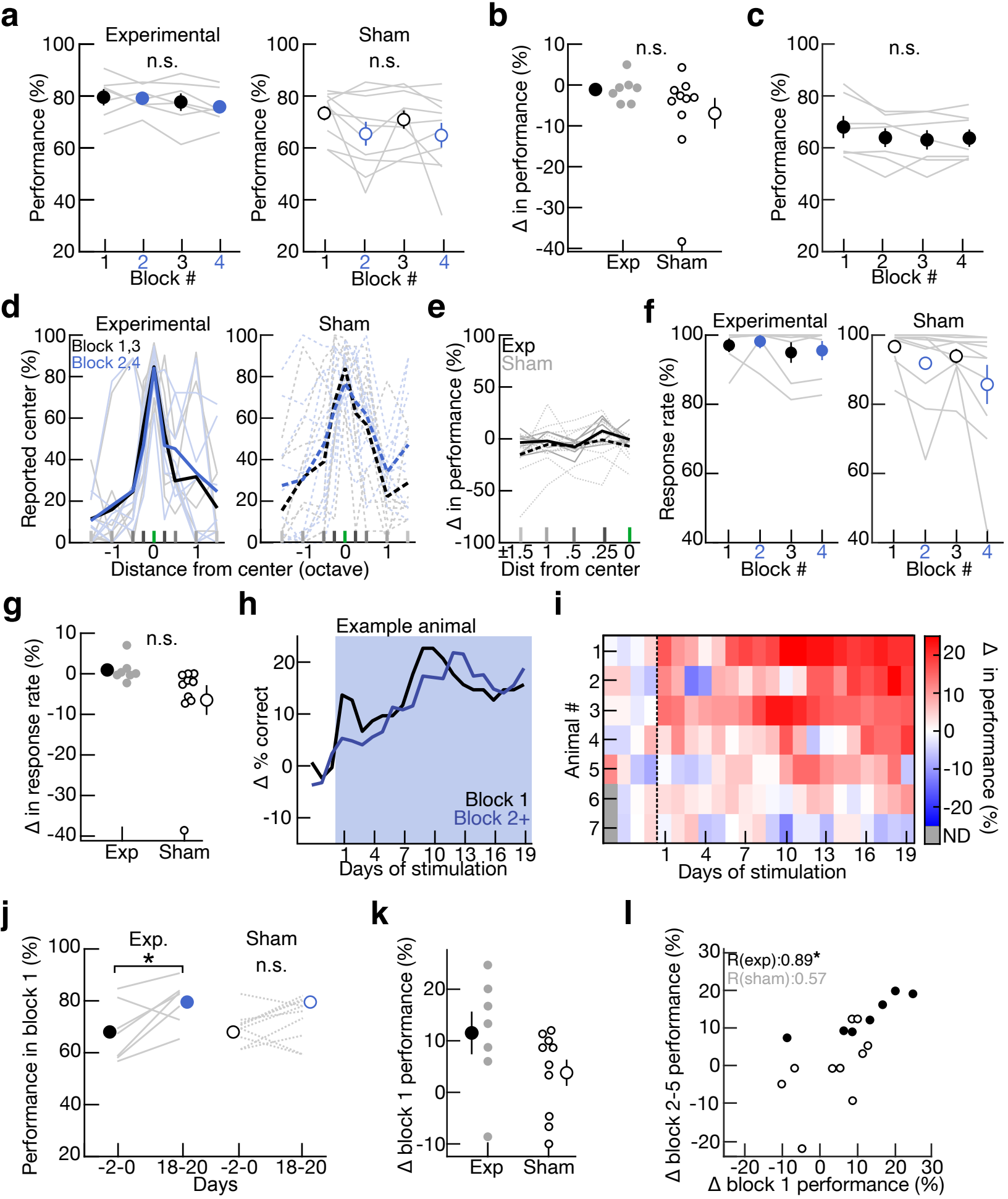
a
Experimental
n.s.
Sham
n.s.
Performance (%)
Block #
b
n.s.
Δ in performance (%)
Exp
Sham
c
n.s.
Performance (%)
Block #
d
Experimental
Sham
Block 1,3
Block 2,4
Reported center (%)
Distance from center (octave)
e
Exp
Sham
Δ in performance (%)
Dist from center
f
Experimental
Sham
Response rate (%)
Block #
g
n.s.
Δ in response rate (%)
Exp
Sham
h
Example animal
Δ % correct
Block 1
Block 2+
Days of stimulation
i
Animal #
Δ in performance (%)
ND
Days of stimulation
j
Exp.
*
Sham
n.s.
Performance in block 1 (%)
Days
k
Δ block 1 performance (%)
Exp
Sham
l
R(exp):0.89*
R(sham):0.57
Δ block 2-5 performance (%)
Δ block 1 performance (%)

Figure 3

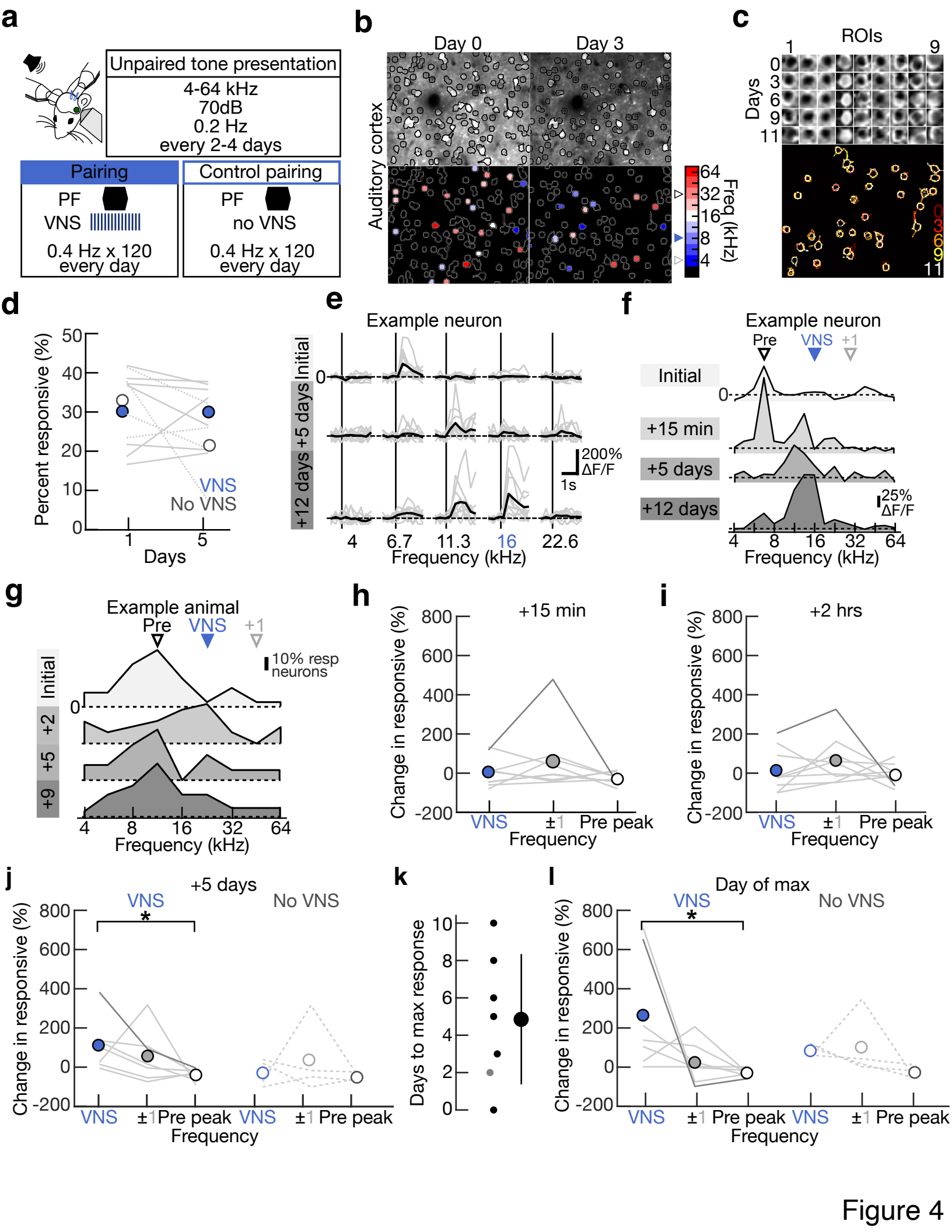
a
Unpaired tone presentation
4-64 kHz
70dB
0.2 Hz
every 2-4 days
Pairing
PF
VNS
0.4 Hz x 120
every day
Control pairing
PF
no VNS
0.4 Hz x 120
every day
b
Day 0
Day 3
Auditory cortex
Freq (kHz)
64
32
16
8
4
c
ROIs
1
9
Days
0
3
6
9
11
d
Percent responsive (%)
Days
VNS
No VNS
e
Example neuron
Initial
+5 days
+12 days
200% ΔF/F
1s
Frequency (kHz)
f
Example neuron
Pre
VNS
+1
Initial
+15 min
+5 days
+12 days
25% ΔF/F
Frequency (kHz)
g
Example animal
Pre
VNS
+1
10% resp neurons
Initial
+2
+5
+9
Frequency (kHz)
h
+15 min
Change in responsive (%)
VNS
±1
Pre peak
Frequency
i
+2 hrs
Change in responsive (%)
VNS
±1
Pre peak
Frequency
j
+5 days
VNS
No VNS
Change in responsive (%)
VNS
±1
Pre peak
VNS
±1
Pre peak
Frequency
k
Days to max response
l
Day of max
VNS
No VNS
Change in responsive (%)
VNS
±1
Pre peak
VNS
±1
Pre peak
Frequency

Figure 4

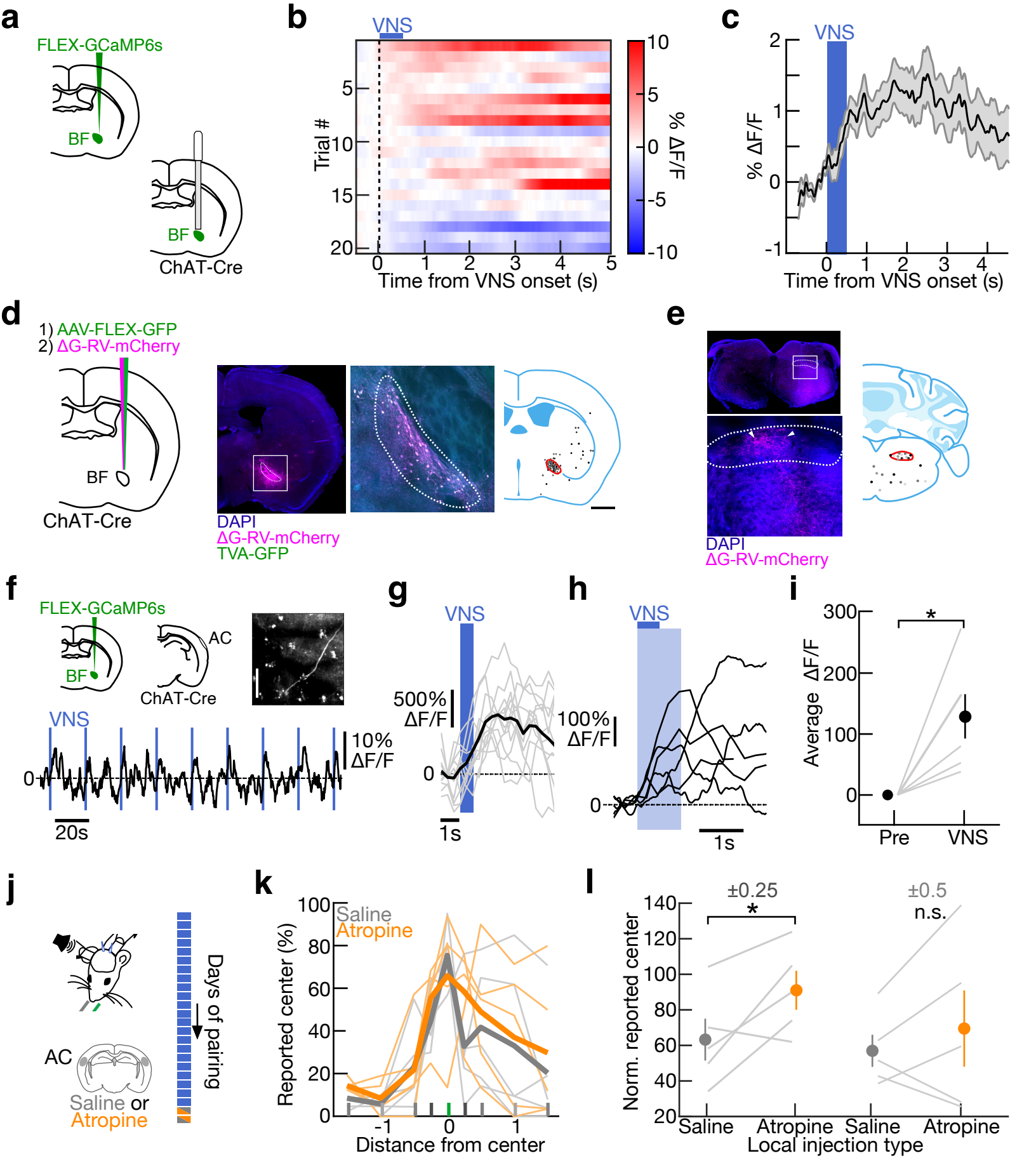
a
FLEX-GCaMP6s
BF
BF
ChAT-Cre
b
VNS
Trial #
Time from VNS onset (s)
% ΔF/F
c
VNS
% ΔF/F
Time from VNS onset (s)
d
1) AAV-FLEX-GFP
2) ΔG-RV-mCherry
BF
ChAT-Cre
DAPI
ΔG-RV-mCherry
TVA-GFP
e
DAPI
ΔG-RV-mCherry
f
FLEX-GCaMP6s
BF
AC
ChAT-Cre
VNS
10% ΔF/F
20s
g
VNS
500% ΔF/F
1s
h
VNS
100% ΔF/F
1s
i
Average ΔF/F
Pre
VNS
j
AC
Saline or Atropine
Days of pairing
k
Saline
Atropine
Reported center (%)
Distance from center
l
±0.25
*
±0.5
n.s.
Norm. reported center
Saline
Atropine
Saline
Atropine
Local injection type

Figure 5

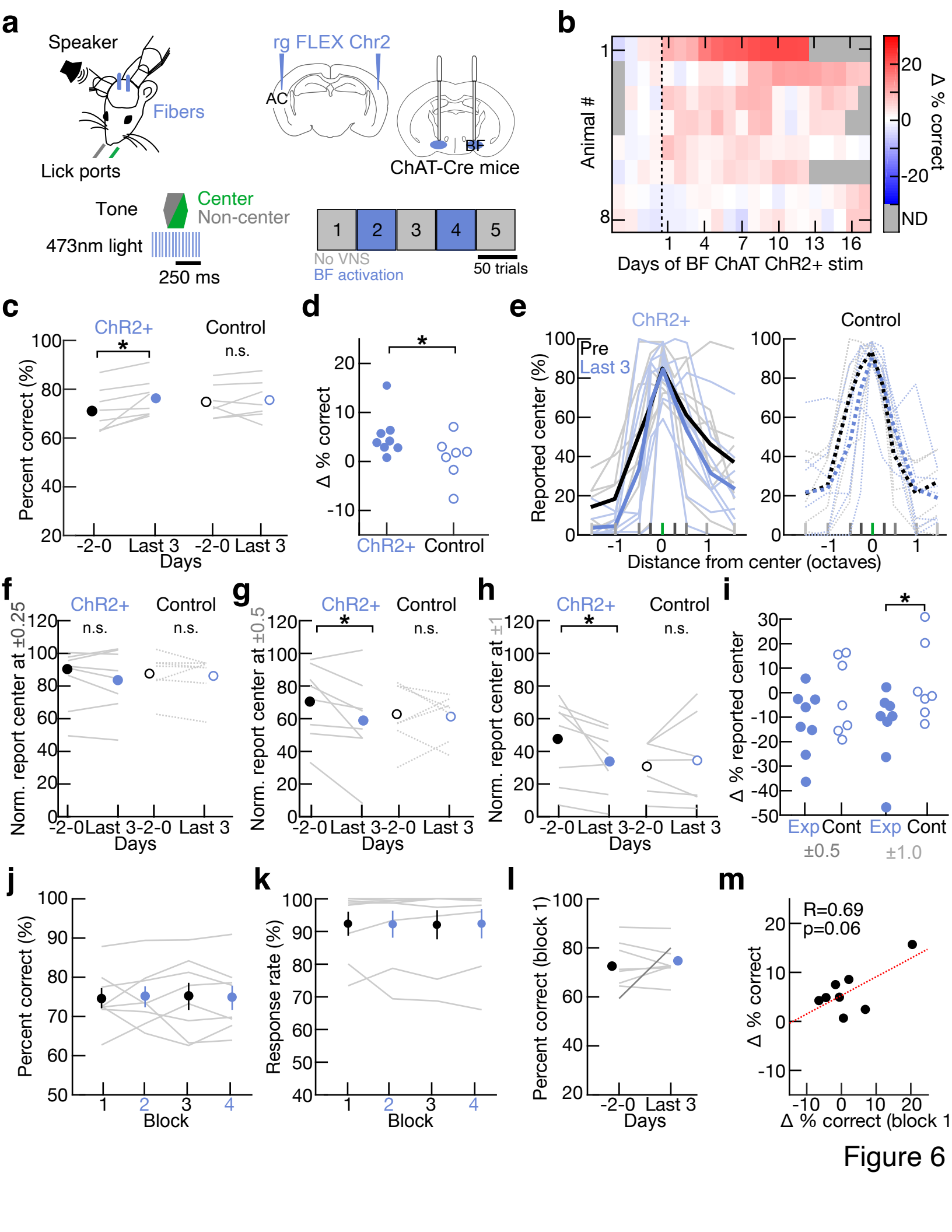
a
Speaker
Fibers
Lick ports
rg FLEX Chr2
AC
BF
ChAT-Cre mice
Tone
Center
Non-center
473nm light
250 ms
1
2
3
4
5
No VNS
BF activation
50 trials
b
Animal #
Days of BF ChAT ChR2+ stim
Δ % correct
ND
c
ChR2+
Control
n.s.
Percent correct (%)
Days
d
Δ % correct
ChR2+
Control
e
ChR2+
Control
Pre
Last 3
Reported center (%)
Distance from center (octaves)
f
ChR2+
Control
n.s.
Norm. report center at ±0.25
Days
g
ChR2+
Control
n.s.
Norm. report center at ±0.5
Days
h
ChR2+
Control
n.s.
Norm. report center at ±1
Days
i
Δ % reported center
Exp
Cont
±0.5
±1.0
j
Percent correct (%)
Block
k
Response rate (%)
Block
l
Percent correct (block 1)
Days
m
R=0.69
p=0.06
Δ % correct
Δ % correct (block 1

Figure 6

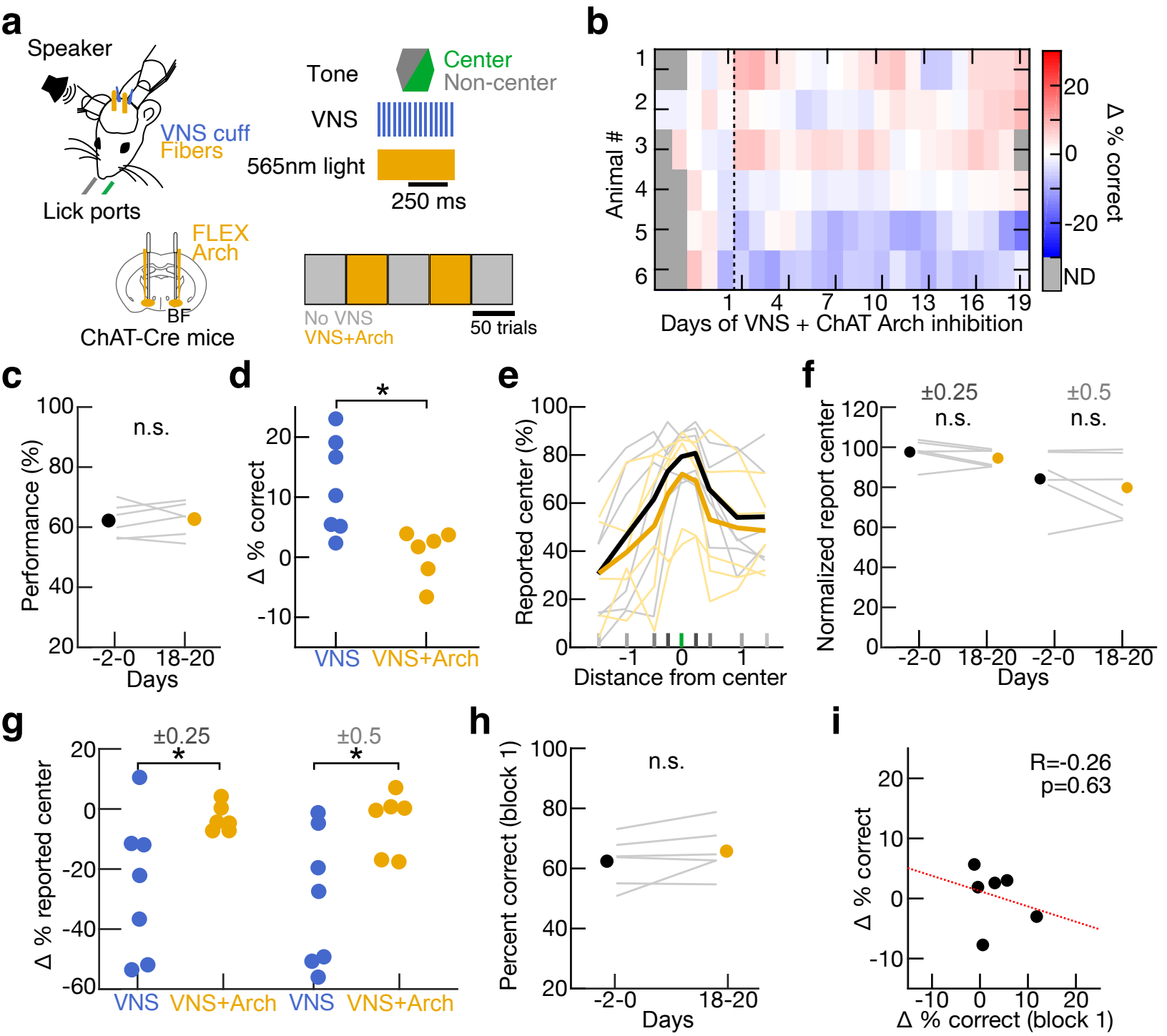
a
Speaker
VNS cuff
Fibers
Lick ports
FLEX
Arch
BF
ChAT-Cre mice
Tone
Center
Non-center
VNS
565nm light
250 ms
No VNS
VNS+Arch
50 trials
b
Animal #
Days of VNS + ChAT Arch inhibition
Δ % correct
ND
c
Performance (%)
n.s.
Days
d
Δ % correct
VNS
VNS+Arch
e
Reported center (%)
Distance from center
f
Normalized report center
±0.25
n.s.
±0.5
n.s.
Days
g
Δ % reported center
±0.25
±0.5
VNS
VNS+Arch
h
Percent correct (block 1)
n.s.
Days
i
R=-0.26
p=0.63
Δ % correct
Δ % correct (block 1)

Figure 7